A Summary of Earlier p+A Experiments' Physics & Results

Workshop on the Physics of p+A Collisions at RHIC
BNL, Jan 7-9, 2013
Mike Leitch, LANL Retired Fellow

Cold Nuclear Matter (CNM) physics

Lessons & Clues from the data:

- shadowing
- initial-state vs final-state
- absorption
- dE/dx from Drell-Yan
- p_T broadening
- Intrinsic Charm
- very small-x shadowing (E665)

FNAL E772/789/866; SPS NA38/50/60;
FNAL E665 (DIS); Cronin expt, …

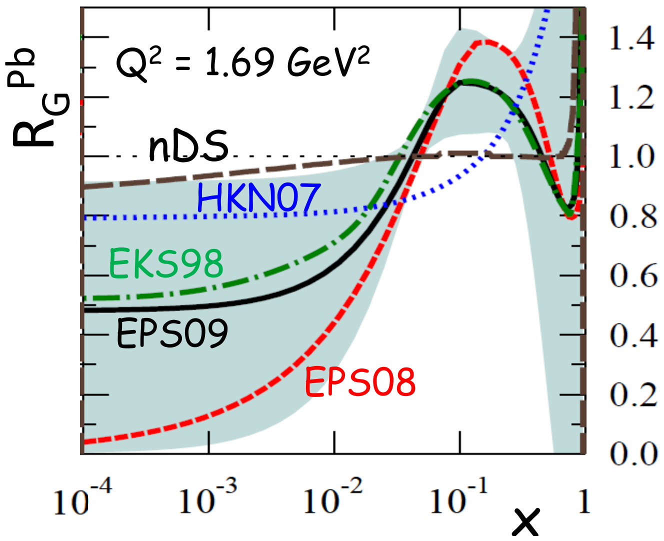

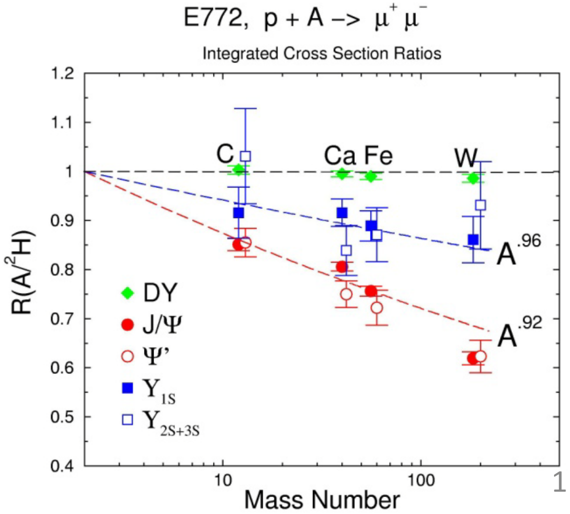

Saturation of Small-x Gluons or Shadowing

Leading twist gluon shadowing, e.g.:

- EPS09 - phenomenological fit to DIS & DY data with large uncertainties, Eskola, Paukkunen, Salgado, JHEP 0904:065,2009
- Also coherence models & higher-twist (HT) shadowing, e.g. Vitev

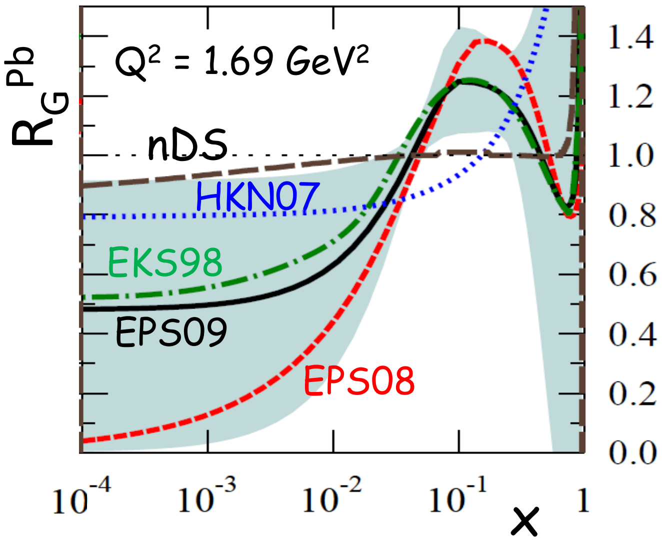

Small-x gluon saturation or Color Glass Condensate (CGC)

- At low-x there are so many gluons that 2→ 1 diagrams become important and deplete the low-x region
- Nuclear amplification: $x_A G(x_A) = A^{1/3} x_p G(x_p)$, i.e. gluon density is ~6x higher in Gold than the nucleon

$$\tau = \ln\left(1/x\right)$$

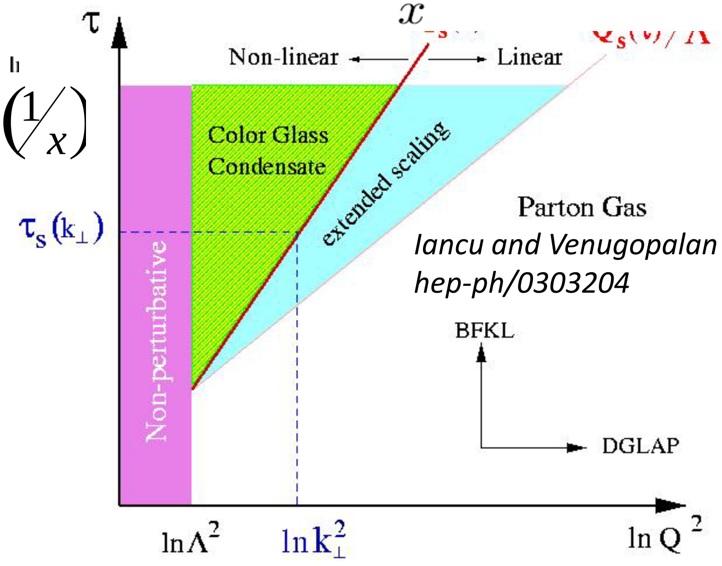

Iancu and Venugopalan hep-ph/0303204

Energy Loss of Partons in Nuclei

Initial-state energy loss

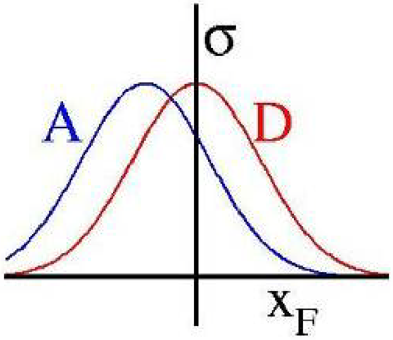

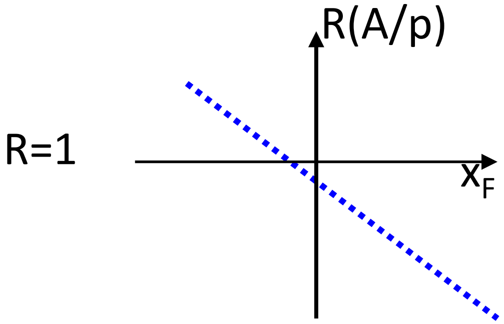

E866/NuSea, 800 GeV, J/Ψ
p+W / p+Be ratio

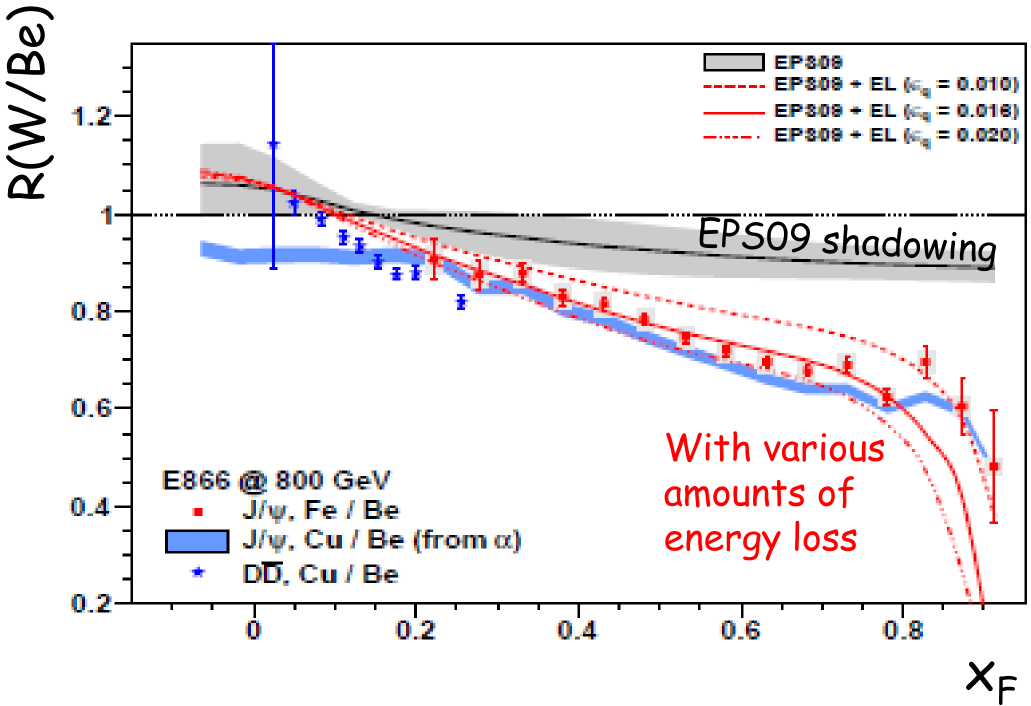

R. Vogt – Jan. 2011

Cronin effect, or p_T broadening from soft initial-state pre-hard-interaction scatterings

Cronin et al., PRD 11, 3105(1975)

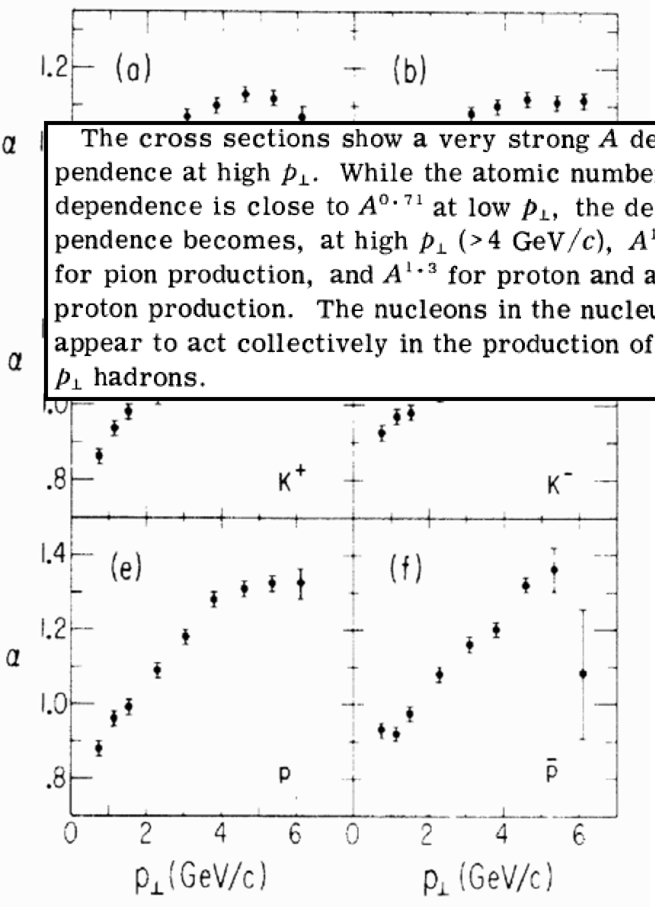

The cross sections show a very strong A dependence at high $p_\perp$. While the atomic number dependence is close to $A^{0.71}$ at low $p_\perp$, the dependence becomes, at high $p_\perp$ (>4 GeV/c), $A^{1.1}$ for pion production, and $A^{1.3}$ for proton and antiproton production. The nucleons in the nucleus appear to act collectively in the production of high-$p_\perp$ hadrons.

FIG. 17. Plots of the power α of the A dependence versus $p_\perp$ for the production of hadrons by 300-GeV protons; (a) π^+, (b) π^-, (c) K^+, (d) K^-, (e) p, and (f) $\bar{p}$.

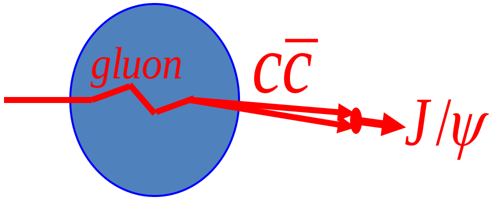

P.B Straub,PRL 68, 452(1992)

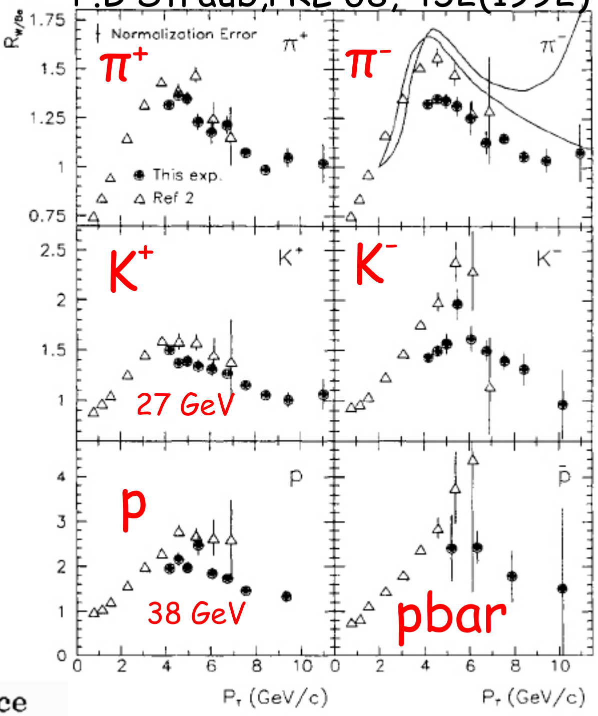

E866/NuSea 800 GeV p+A

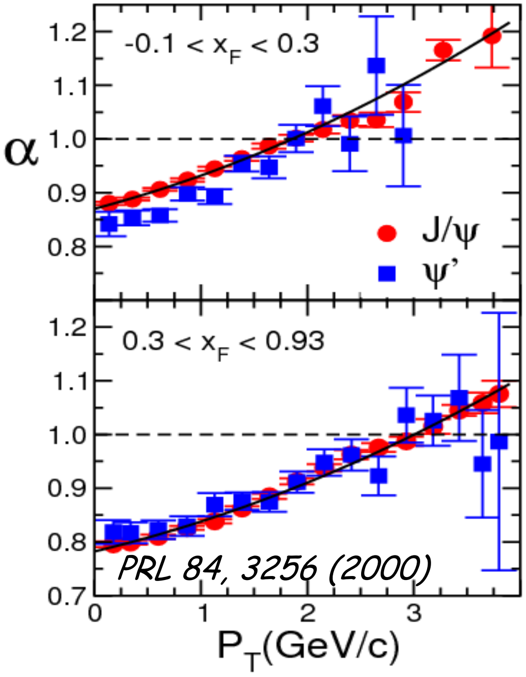

PRL 84, 3256 (2000)

Lessons and Clues from the Data

Cronin expt.

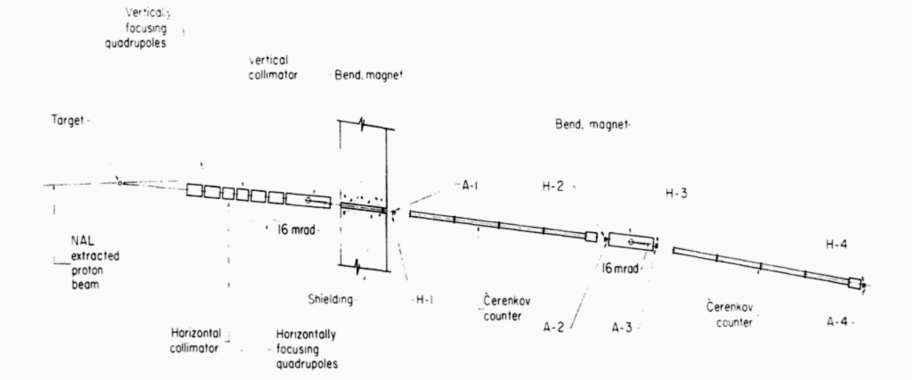

E866/NuSea

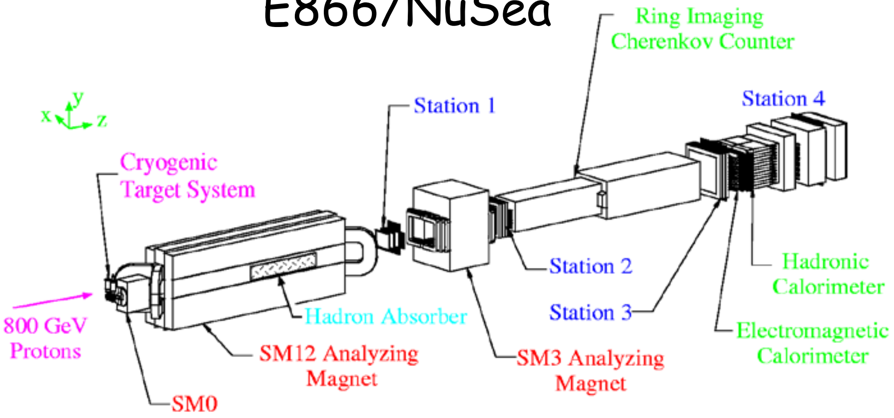

NA50

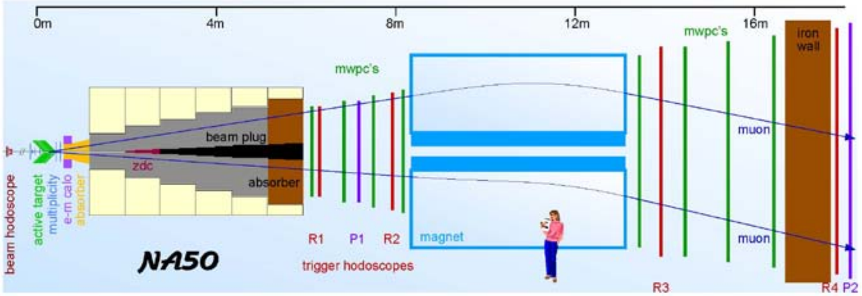

HERA-B

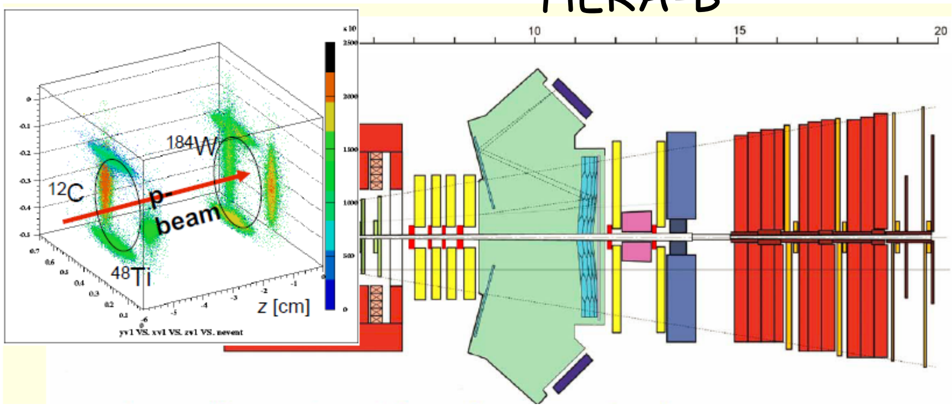

Suppression Not Universal vs x_2 as Expected for Shadowing

PHENIX, E866, NA3 J/ψ Comparison

$$\sigma_{pA} = \sigma_{pp} A^{\alpha}$$

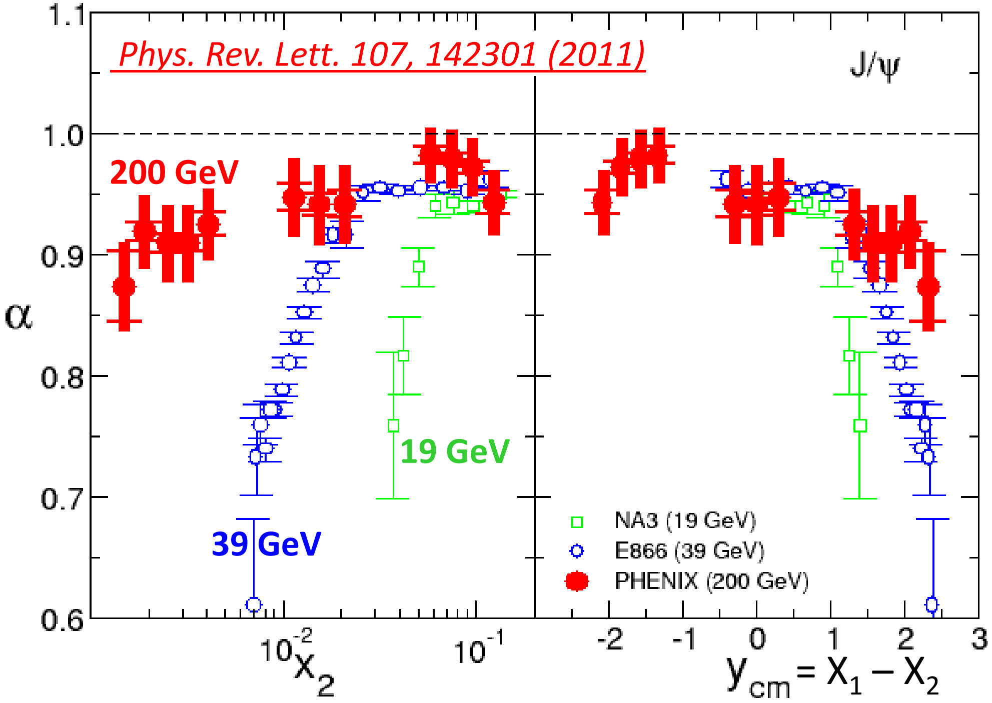

(x_2 is x in the nucleus)

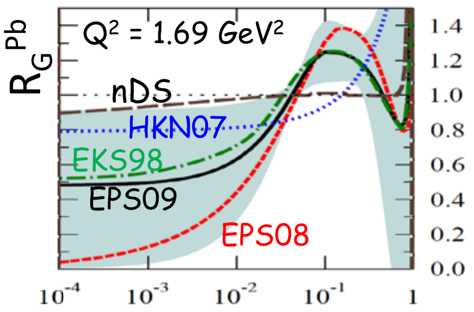

Closer to scaling with x_F or rapidity

- initial-state gluon energy loss?

Energy loss of incident gluon shifts effective x_F and produces nuclear suppression which increases with x_F

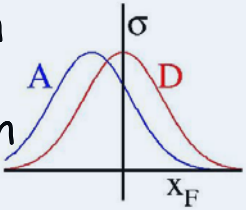

- or gluon saturation?

Gluon saturation from non-linear gluon interactions for the high density at small x; amplified in a nucleus.

Fermilab E789: $D^0 \rightarrow K\pi$ and $B \rightarrow J/\psi\ X$
(charm & beauty using silicon vertex detector)

Dimuon spectrometer
+

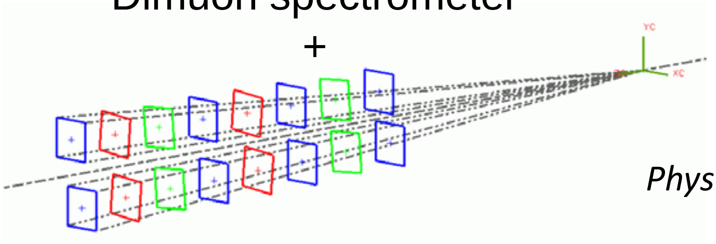

16-plane, 50μm pitch/8.5k strip silicon vertex detector

B -> J/ψ + X

Phys. Rev. Lett. 74, 3118 (1995)

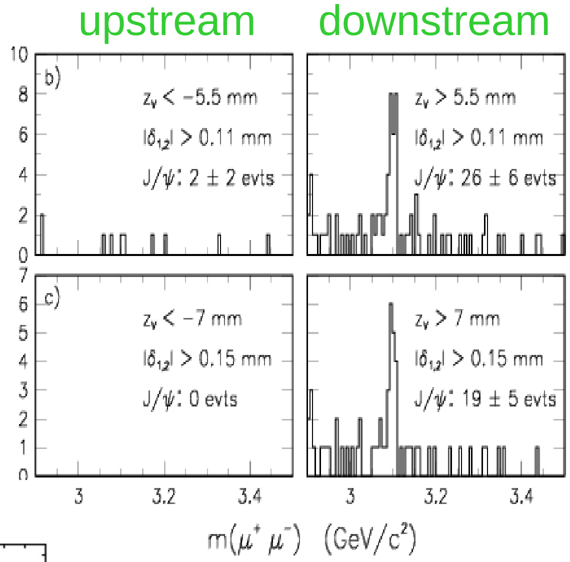

Phys. Rev. Lett. 72, 2542 (1994)

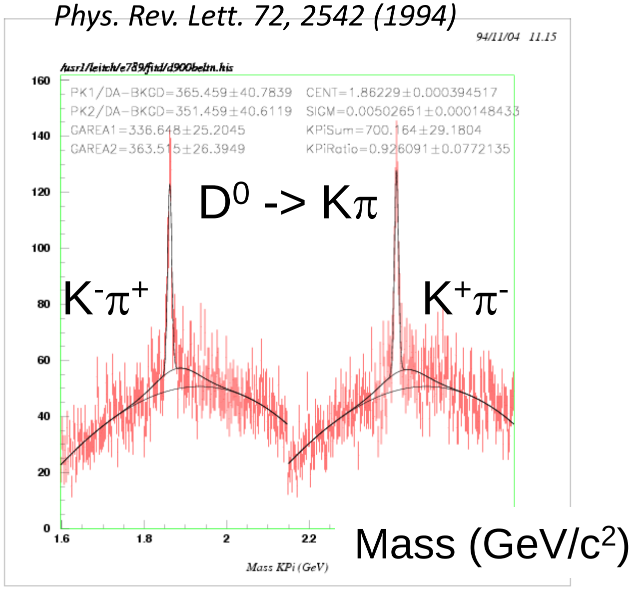

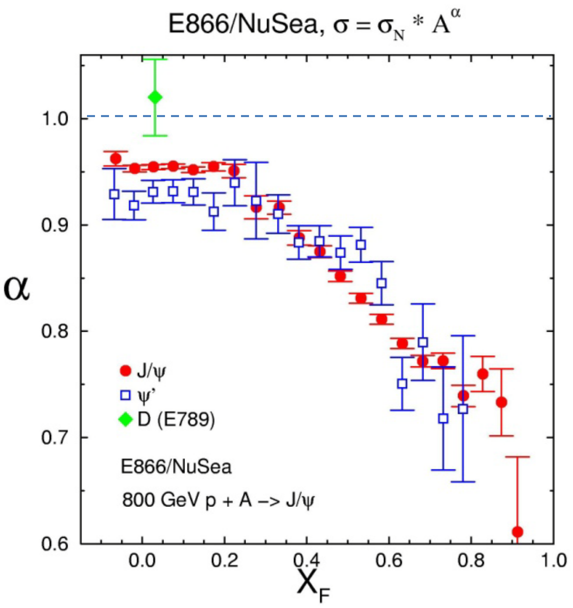

Compare closed and open charm to isolate initial-state CNM effects

Comparing Open & Closed Charm
Isolating Initial-state Effects

E866/NuSea 800 GeV p+A

Open-charm p+A nuclear dependence (single-μ $p_T > 1$ GeV/c) – very similar to that of J/Ψ:

- implies that dominant effects are in the initial state
  - e.g. dE/dx, CGC (since shadowing disfavored by lack of x_2 scaling)
- weaker open-charm suppression at y=0 attributed to lack of absorption for open charm

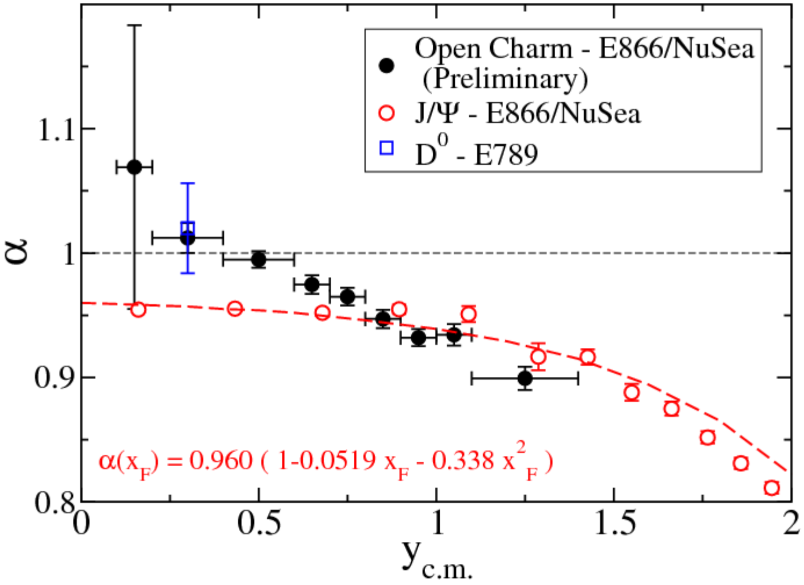

follow this example at RHIC

Absorption at mid-rapidity, J/ψ & ψ′ in Fixed Target Measurements

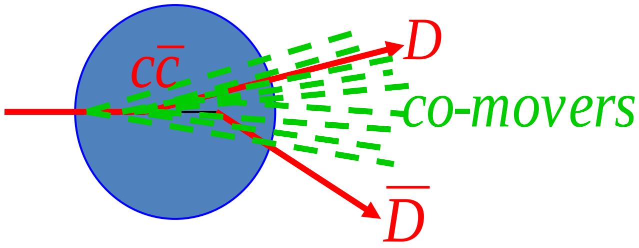

Absorption (or dissociation) of J/ψ or pre-J/ψ ($c\bar{c}$) as they exit nucleus into two D mesons, by nucleus or co-movers

$$\sigma_{pA} = \sigma_{pp} A^{\alpha}$$

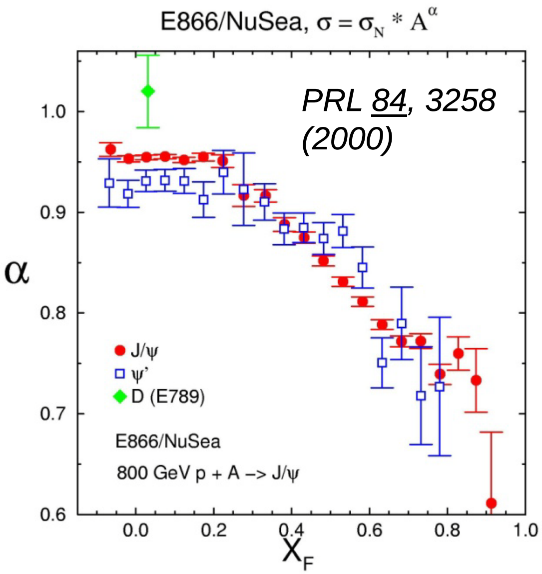

Power law parameterization $\sigma = \sigma_N * A^{\alpha}$

$\alpha = 0.954 \pm 0.003$ E866/NuSea @ $x_F=0$

$\alpha = 0.941 \pm 0.004$ NA50, QM04

Absorption model parameterization (from pA)

$\sigma_{J/\psi} = 4.18 \pm 0.35$ mb NA50 QM05

$\sigma_{\psi'} = 7.6 \pm 1.1$ mb

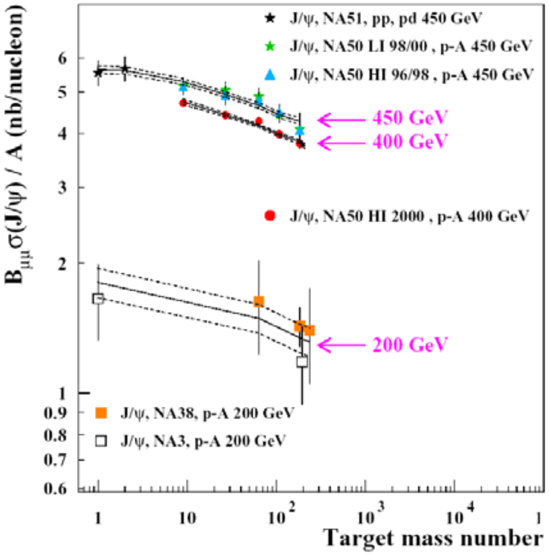

Absorption or Dissociation of J/ψ after correcting for shadowing

Energy Dependence; after corrections for EKS98 shadowing

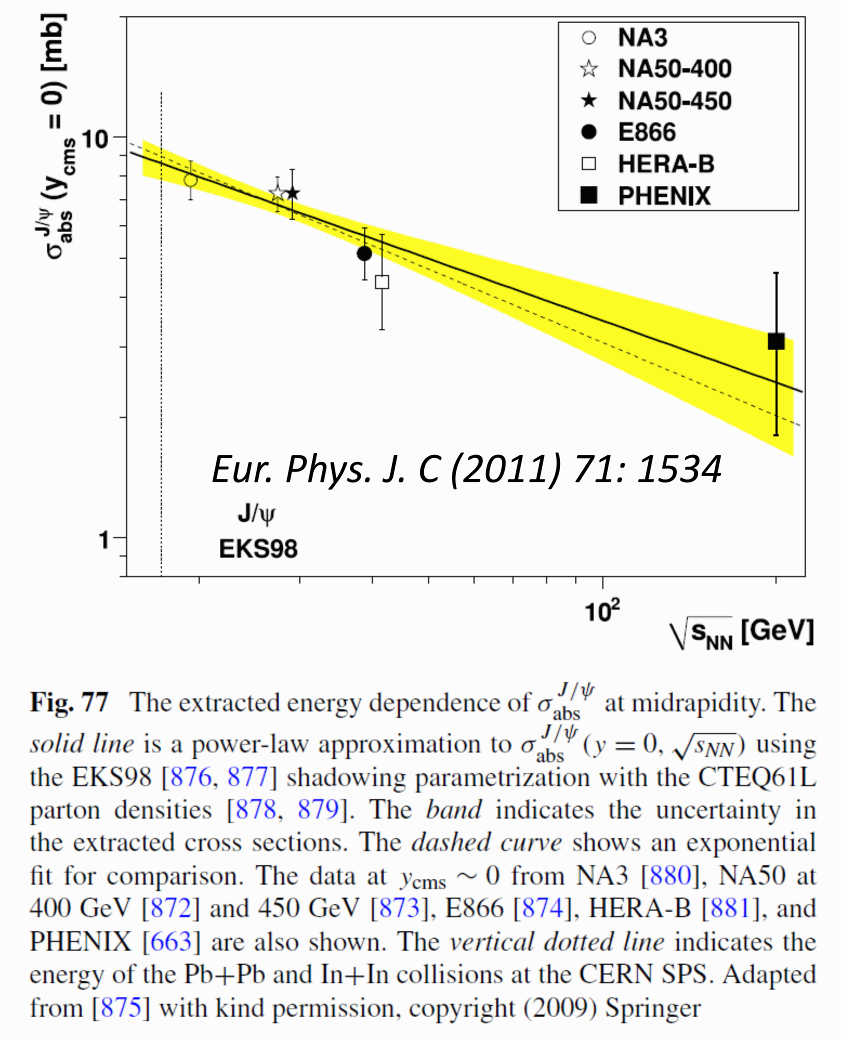

Eur. Phys. J. C (2011) 71: 1534

Fig. 77 The extracted energy dependence of $\sigma_{abs}^{J/\psi}$ at midrapidity. The *solid line* is a power-law approximation to $\sigma_{abs}^{J/\psi}(y = 0, \sqrt{s_{NN}})$ using the EKS98 [876, 877] shadowing parametrization with the CTEQ61L parton densities [878, 879]. The *band* indicates the uncertainty in the extracted cross sections. The *dashed curve* shows an exponential fit for comparison. The data at $y_{cms} \sim 0$ from NA3 [880], NA50 at 400 GeV [872] and 450 GeV [873], E866 [874], HERA-B [881], and PHENIX [663] are also shown. The *vertical dotted line* indicates the energy of the Pb+Pb and In+In collisions at the CERN SPS. Adapted from [875] with kind permission, copyright (2009) Springer

Apparent absorption vs x_F; after EKS98 shadowing is removed

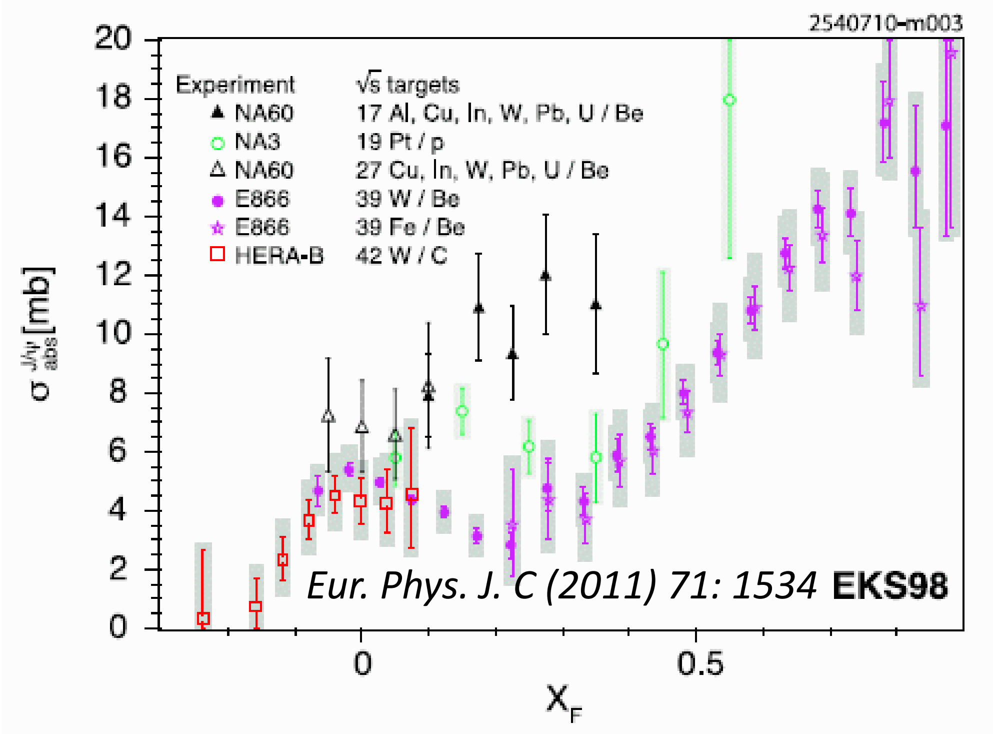

Eur. Phys. J. C (2011) 71: 1534 **EKS98**

ψ′ absorbed more than J/ψ near x_F = 0

Meson	M(GeV)	R(Fm)	BE (MeV)
J/Ψ	3.1	.45	~640
Ψ′	3.7	.88	~52

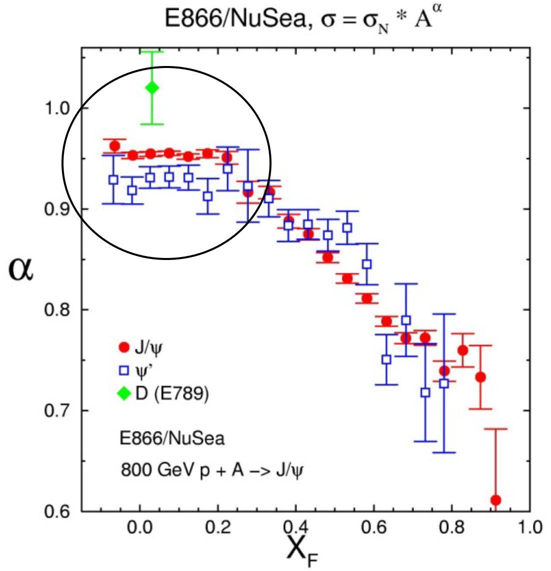

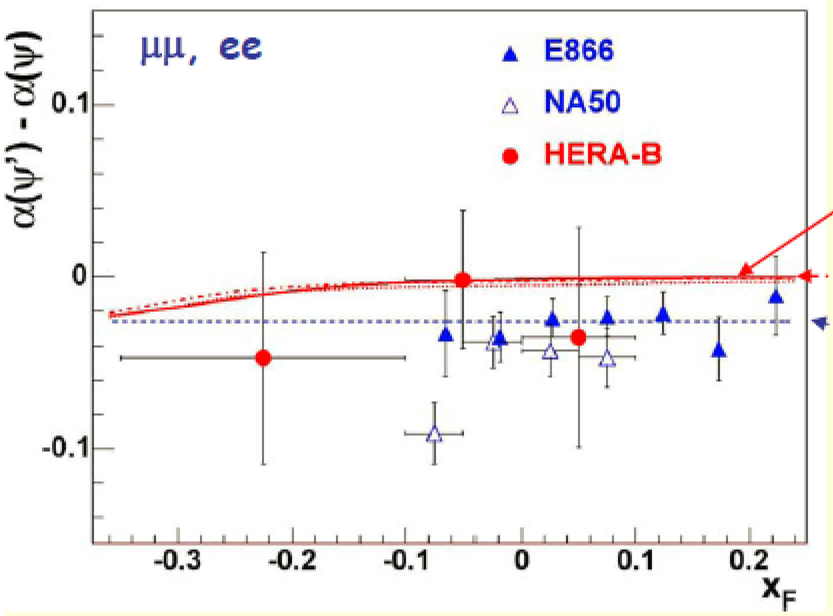

A-dependence: $\Delta\alpha(x_F) = \alpha' - \alpha$

CEM for color-1 nuclear absorption

NRQCD for color-1 & -8 nuclear absorption

fit with const: Δα(E866)=-0.026±0.005

All consistent with no x_F dependence.
We use average of E866 and NA50:
Δα(E866, NA50)=-0.030±0.004

4/4/2006 Hermann Kolanoski HU Berlin - HERA-B Results - BNL060404

Contrasting ϒ's with J/ψ's

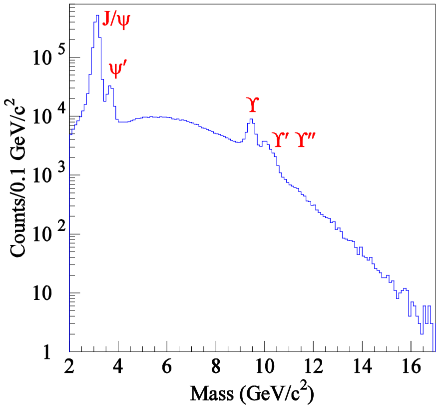

$\sqrt{S}$ =39 GeV (E772 & E866)

- less absorption
- not in shadowing region (large x_2)
- similar p_T broadening

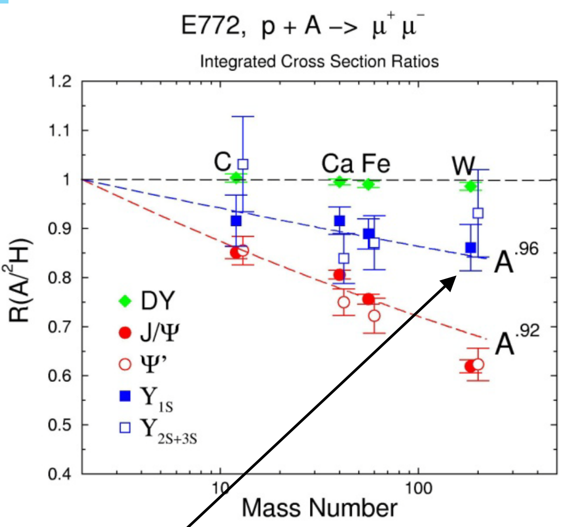

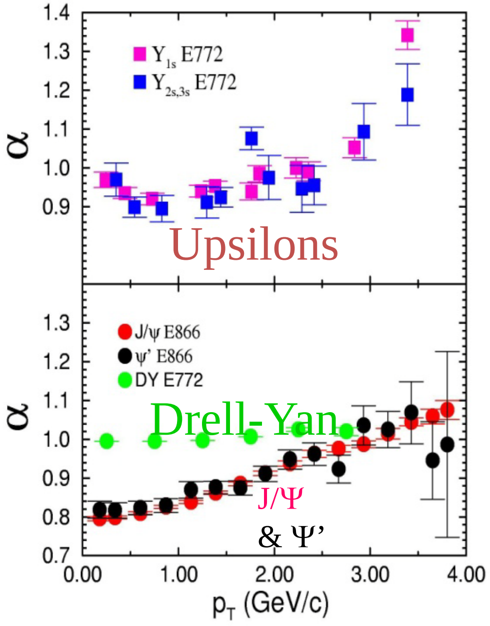

But careful: ϒ suppression is from data for x_F < 0 or x_2 > 0.2 (in the EMC region)

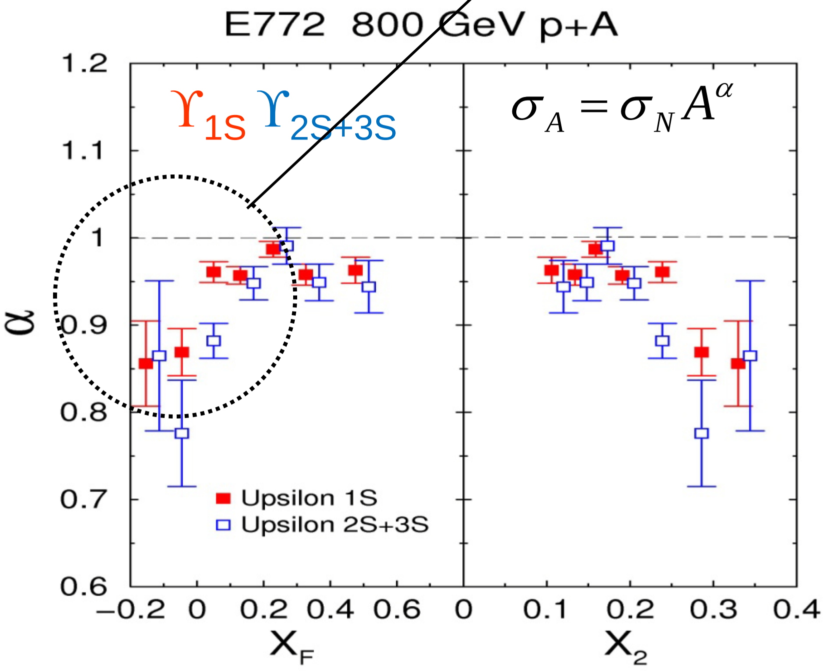

Drell-Yan

$$pN \to \mu^+\mu^- X$$

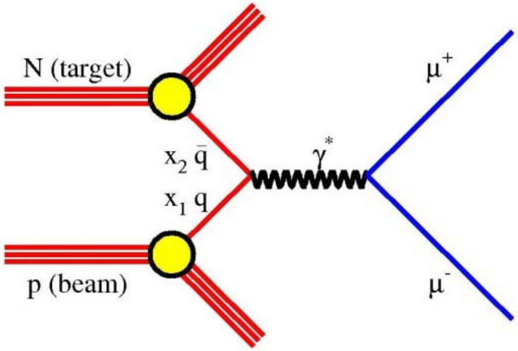

Drell-Yan from E772/E789/E866 at Fermilab

$$pN \to \mu^+\mu^- X$$

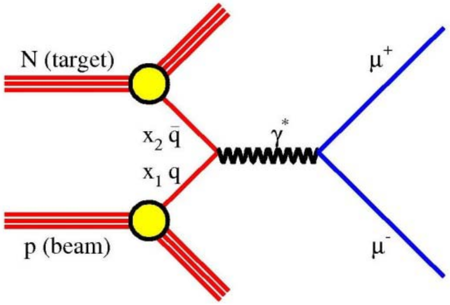

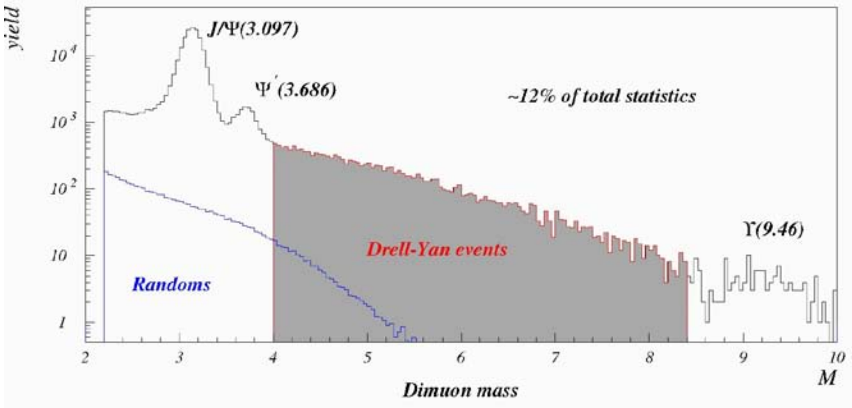

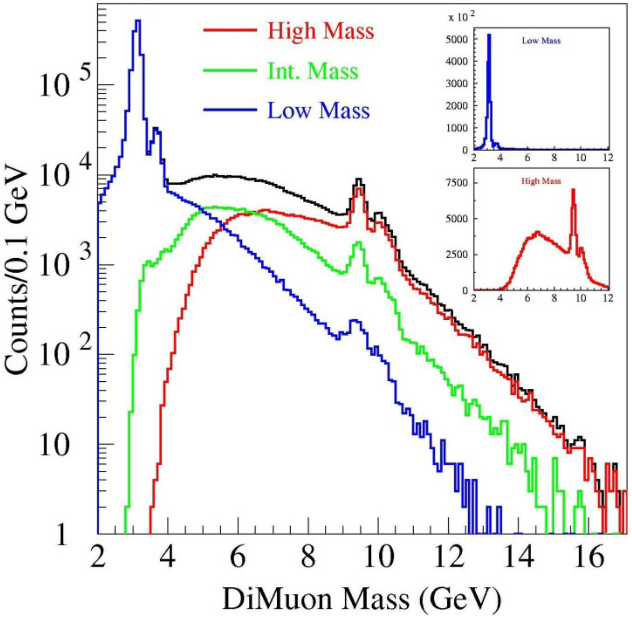

Phys. Rev. Lett. 83, 2304 (1999)

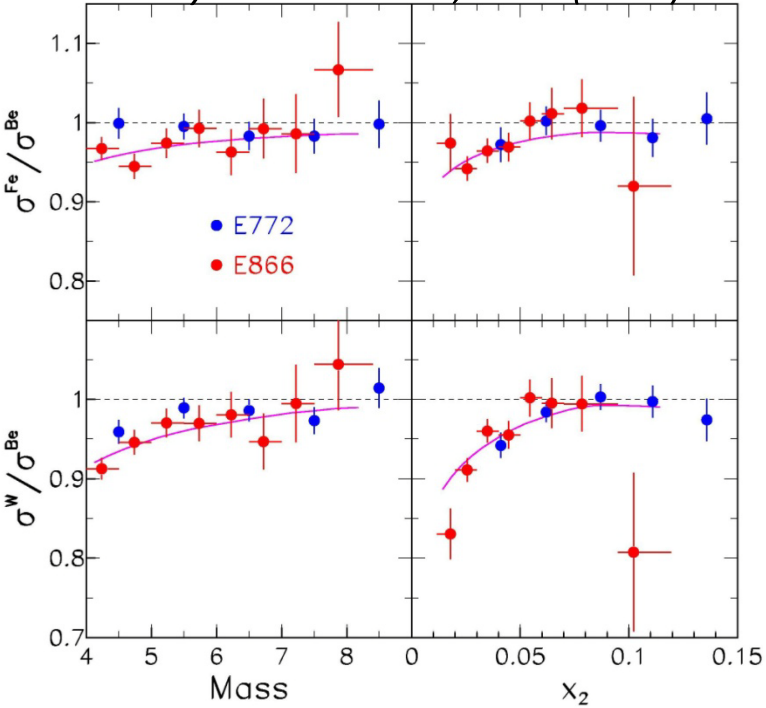

Quark Energy Loss from Drell-Yan data
Two ways

assuming EKS Shadowing

Phys. Rev. Lett. 83, 2304 (1999)

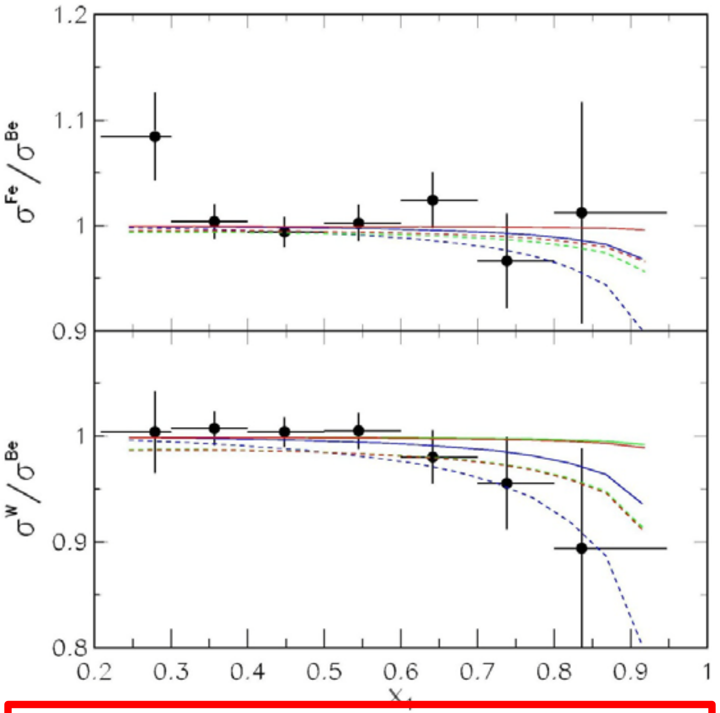

- Gavin and Milana $\Delta E < 0.14\,\%/\mathrm{fm}$
- Brodsky and Hoyer $\Delta E < 0.44\,\mathrm{GeV/fm}$
- Baier et al. $\Delta E < (0.046\,\mathrm{GeV/fm^2}) \times L^2$

assuming Kopeliovich Shadowing

Johnson, Kopeliovich et al., PRL <u>*86*</u>*, 4483 (2001)*

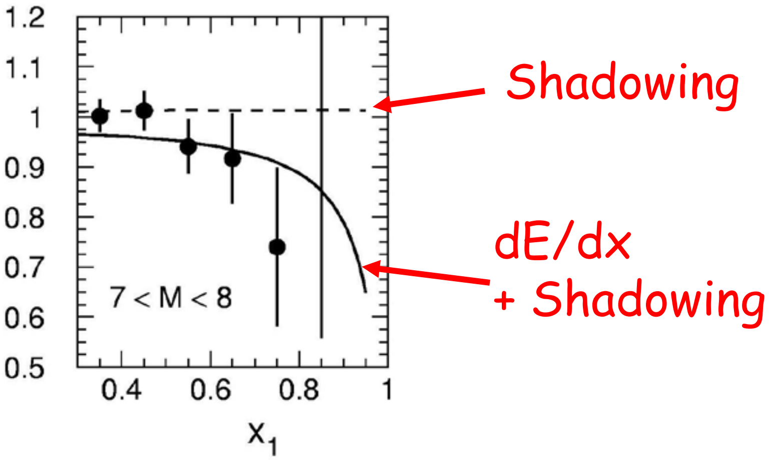

Analysis of our p-A Drell-Yan data using the Kopeliovich model.

$dE/dx = 2.32 \pm 0.52 \pm 0.5$ GeV/fm

Confusion due to having both shadowing and dE/dx contributing to Drell-Yan suppression for measurements at this energy

Drell-Yan to constrain parton energy loss in CNM

FNAL E906/Seaquest – Drell-Yan

Drell-Yan

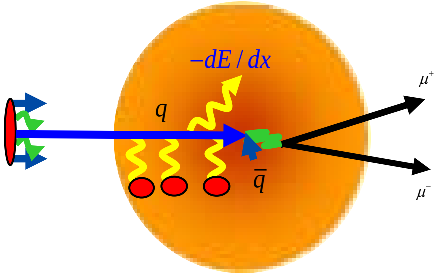

In E906 at 120 GeV, nuclear suppression in Drell-Yan should only be from dE/dx ($x_2 > 0.1$)

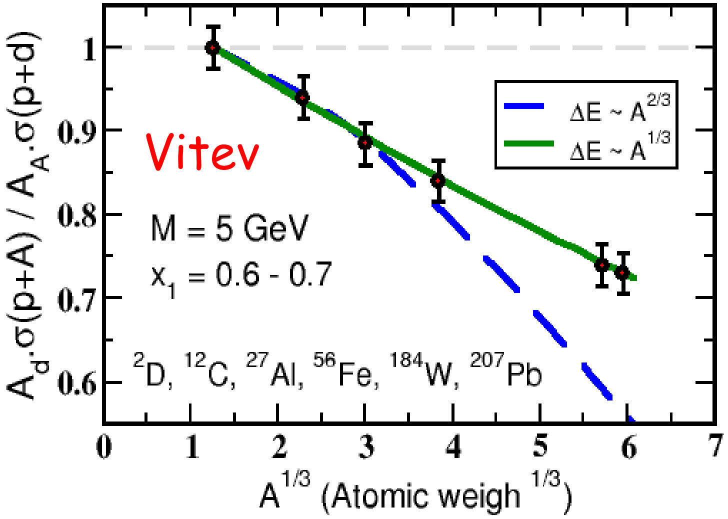

$$\frac{\Delta E}{E} \propto \frac{\mu^2 L^2}{\lambda_g} \, \frac{\ln E / Q_0}{E}$$

$$\frac{\Delta E}{E} \propto \frac{L}{\lambda_g} \, \ln \frac{E}{Q_0}$$

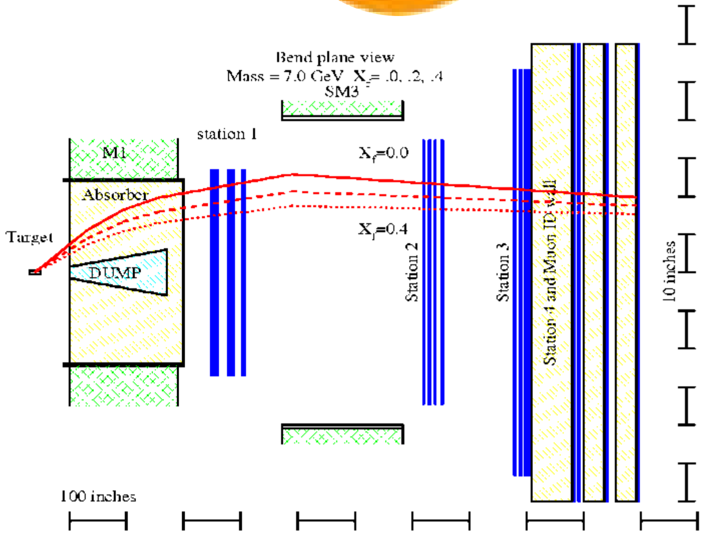

Distinguish radiative from collisional (L^2 vs L)

See Paul Reimer's talk

Transverse Momentum Broadening

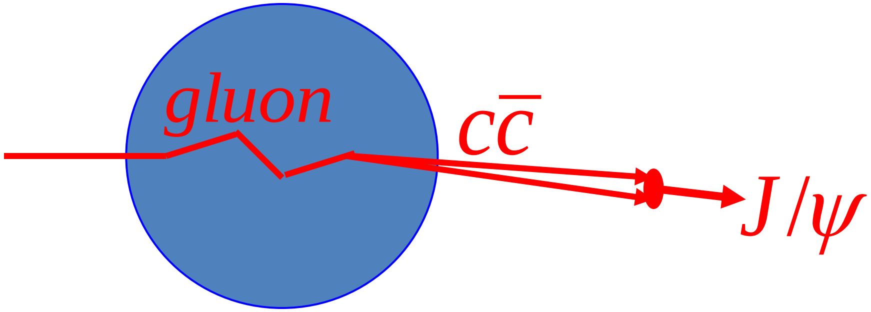

Transverse Momentum Broadening – DY, J/ψ, Upsilon

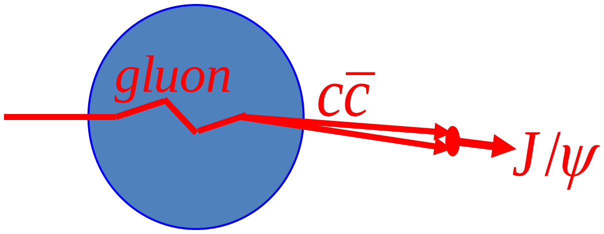

Initial-state gluon multiple scattering causes p_T broadening (or Cronin effect)

$$\sigma_A = \sigma_N A^{\alpha}$$

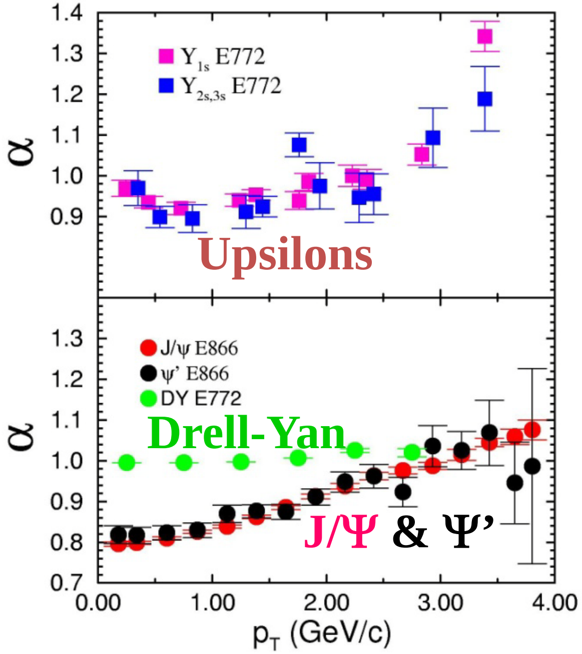

PRL 96, 012304 (2006)

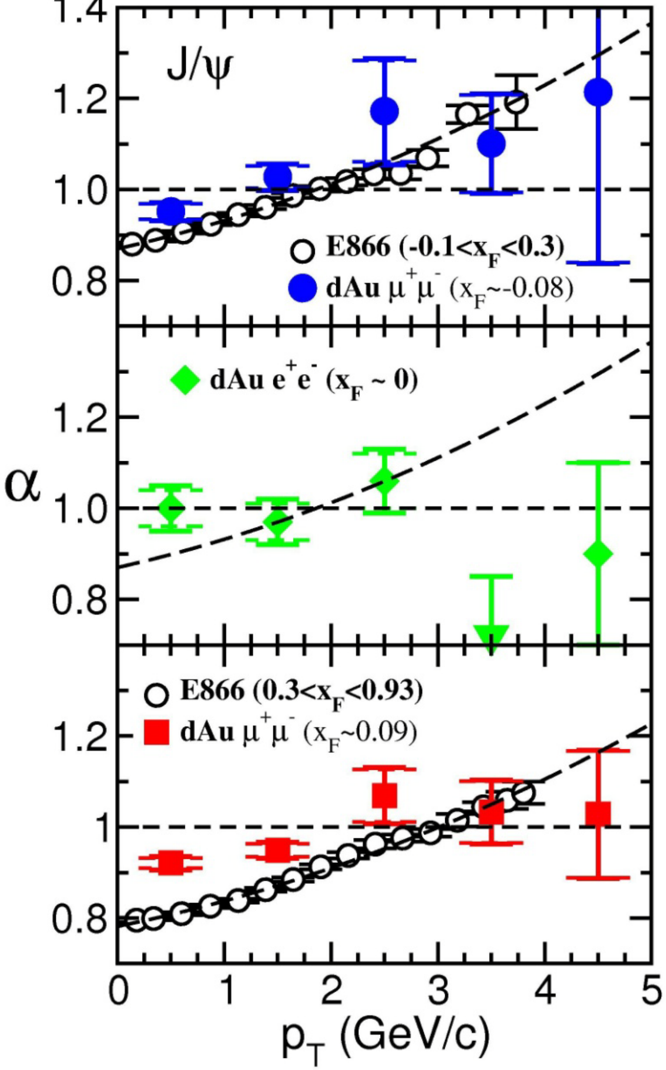

High x_2 ~ 0.09

PHENIX 200 GeV results show p_T broadening comparable to that at lower energy ($\sqrt{s}=39$ GeV in E866/NuSea)

Low x_2 ~ 0.003

Systematics of P_T Broadening
E866/NuSea

$$\Delta\left\langle p_T^2 \right\rangle = \Delta\left\langle p_T^2 \right\rangle_A - \Delta\left\langle p_T^2 \right\rangle_D$$

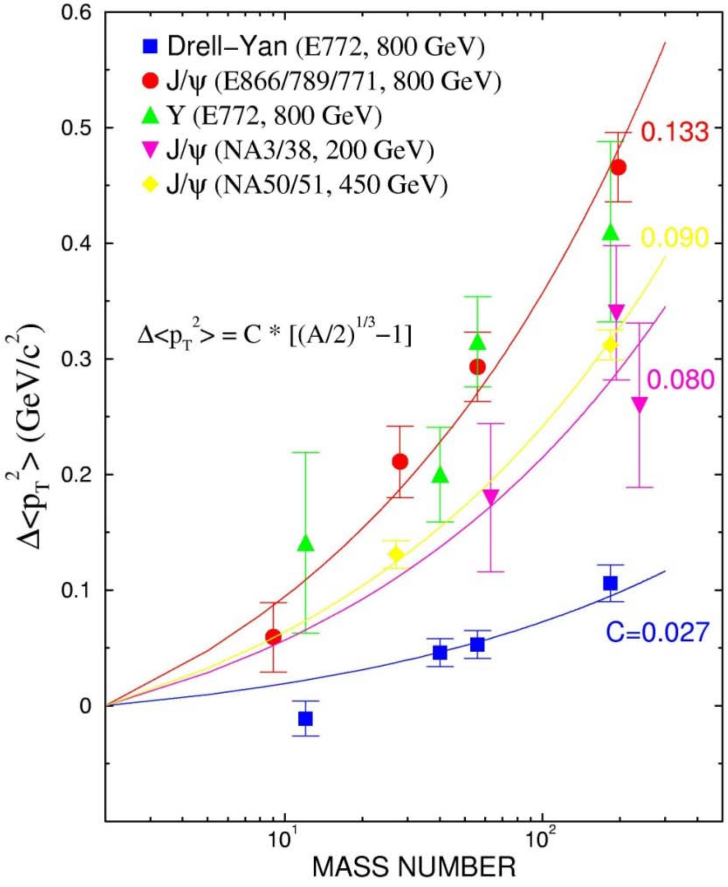

$$\Delta\left\langle p_T^2 \right\rangle = C * \left[\left(A/2\right)^{1/3} - 1\right]$$

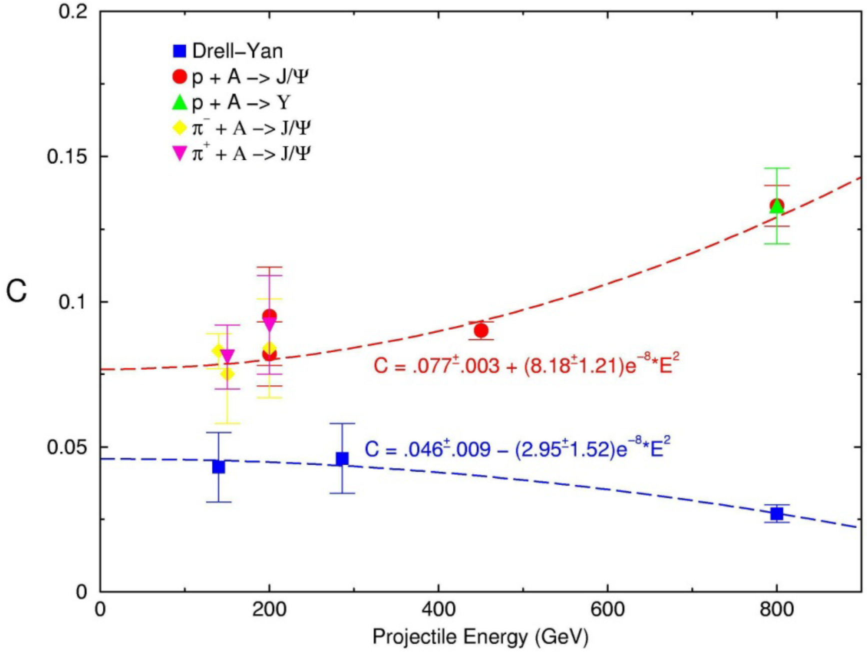

P_T Broadening for different energies and probes – other data

E537: 125 GeV pbar,π^- J/ψ

PRL 60, 2121 (1988)

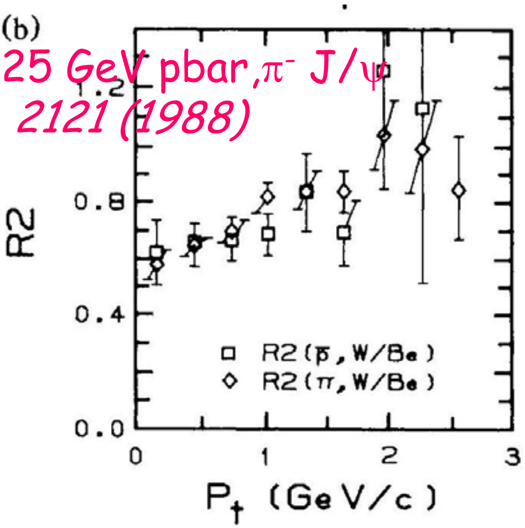

E288 400 GeV p DY

PRD 23, 604 (1981)

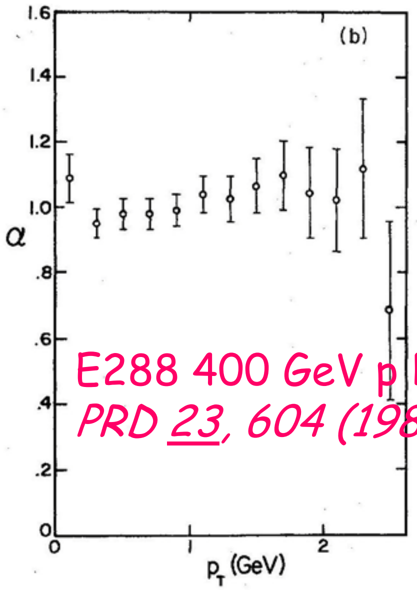

NA10: 140,286 GeV π^- DY

PLB 193, 368 (1987)

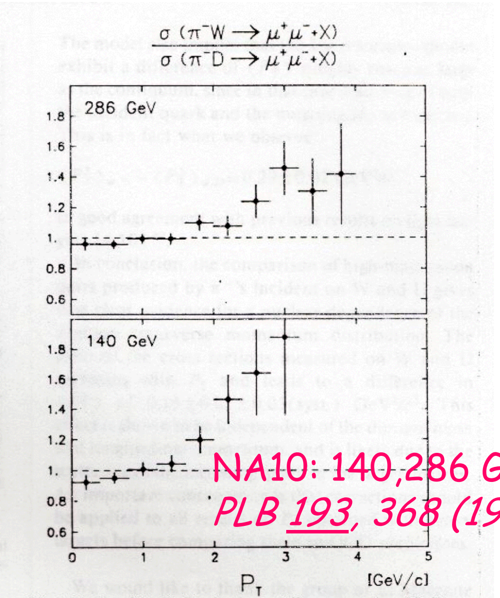

Fig. 1. Ratios of the P_T distributions of dimuons produced in W and D. The W and D samples are normalized to the same number of events. Only statistical uncertainties are shown.

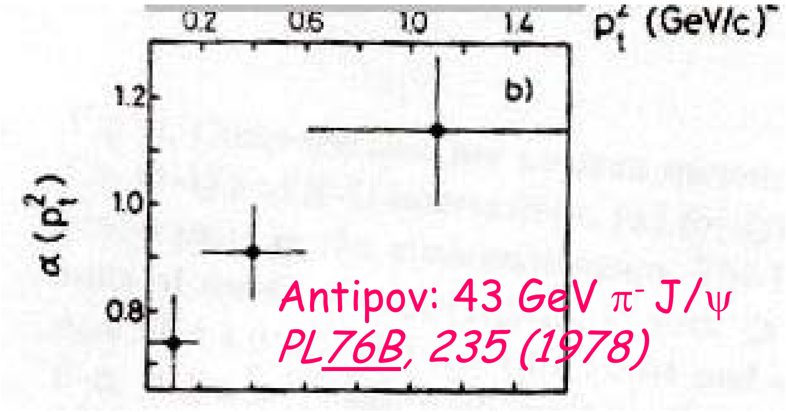

Antipov: 43 GeV π^- J/ψ

PL76B, 235 (1978)

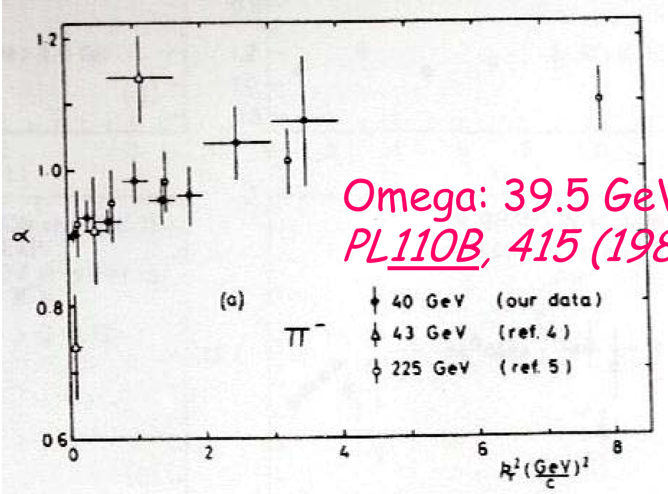

Omega: 39.5 GeV π^- J/ψ

PL110B, 415 (1982)

Deuteron vs the Proton

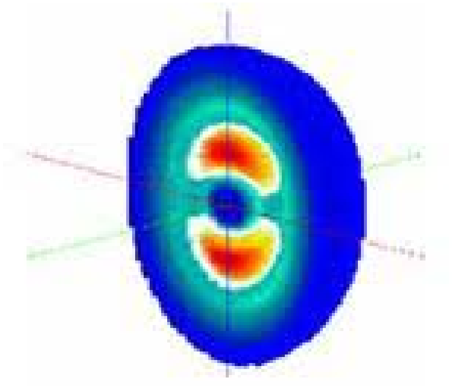

Deuteron is very weakly bound & not a typical nucleus in terms of CNM effects

- Binding energies:
    - D – 2.22 MeV
    - Alpha – 28.3 MeV

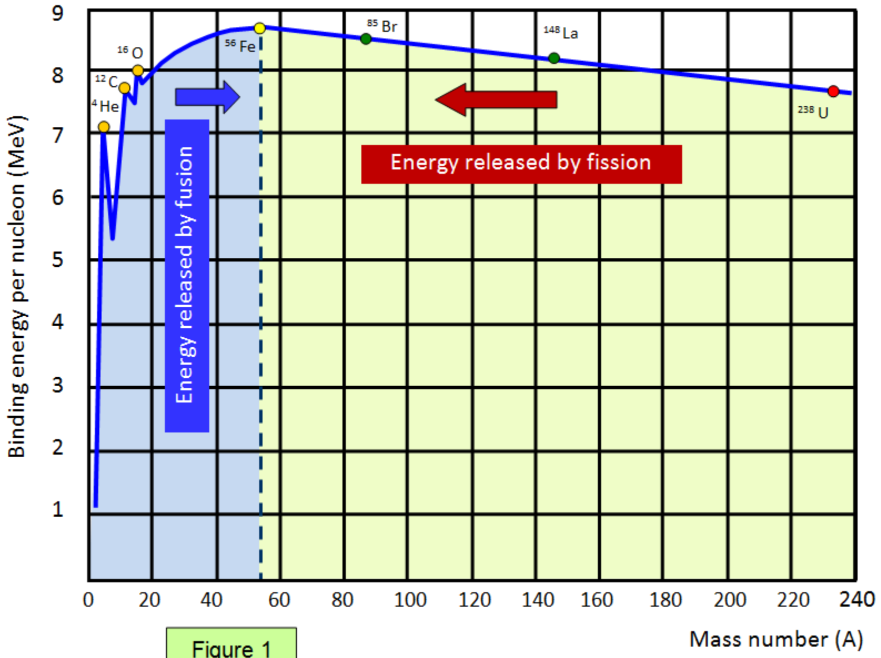

Figure 1

J/ψ Nuclear dependence weaker than expected for Deuterium/Hydrogen !

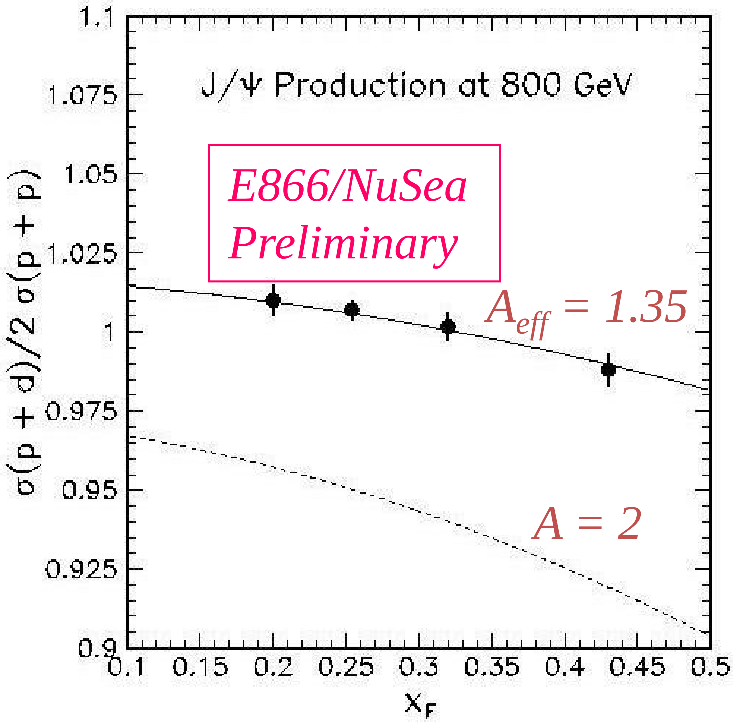

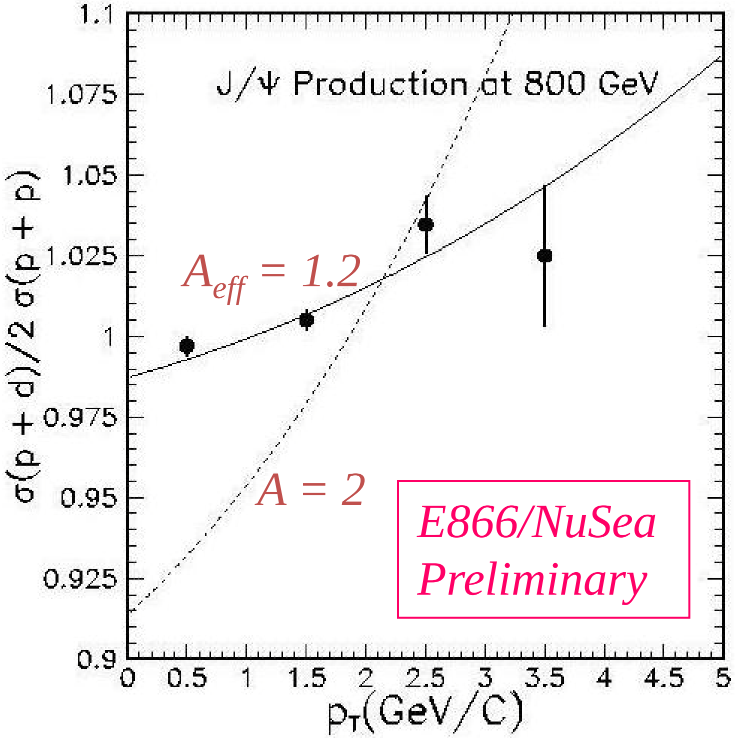

Nuclear dependence in deuterium seems to follow the systematics of larger nuclei, but with an effective, A_{eff}, smaller than the A=2 of deuterium

From fits to E866/NuSea
p + Be, Fe, W data: $\sigma_{pA} \sim \sigma_{pp} A^{\alpha}$

$$\alpha(x_F) \propto 1 - 0.052 x_F - 0.034 x_F^2$$

$$\alpha(p_T) \propto 0.06 p_T + 0.011 p_T^2$$

Intrinsic Charm

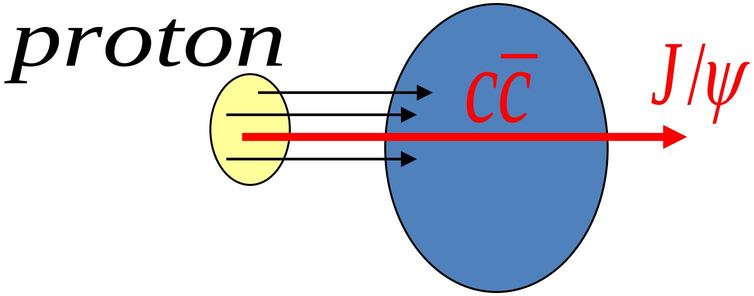

Intrinsic charm components of incident proton produce J/ψ at large x_F. $A^{2/3}$ dependence from surface stripping of proton's light quarks (Brodsky)

Intrinsic charm contribution to Quarkonia

At large x_F (≥ 0.5) intrinsic $c\bar{c}$ components of the projectile proton can dominate the production of charm pairs

- $A^{2/3}$ dependence via surface stripping of light quarks to free charm pair component

Vogt, Brodsky, Hoyer, NP B360, 67 (1991)
(also includes absorption and shadowing)

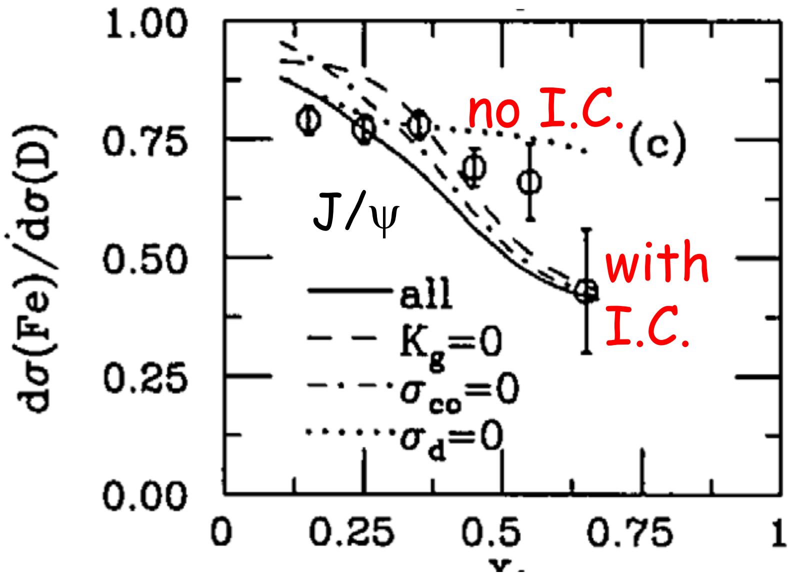

No conclusive evidence for IC:
"IC constrained to be from zero (no IC) to a level 2-3 times larger than previous model estimates"

Pumplin, Lai, Tung, PRD 75, 054029 (2007)

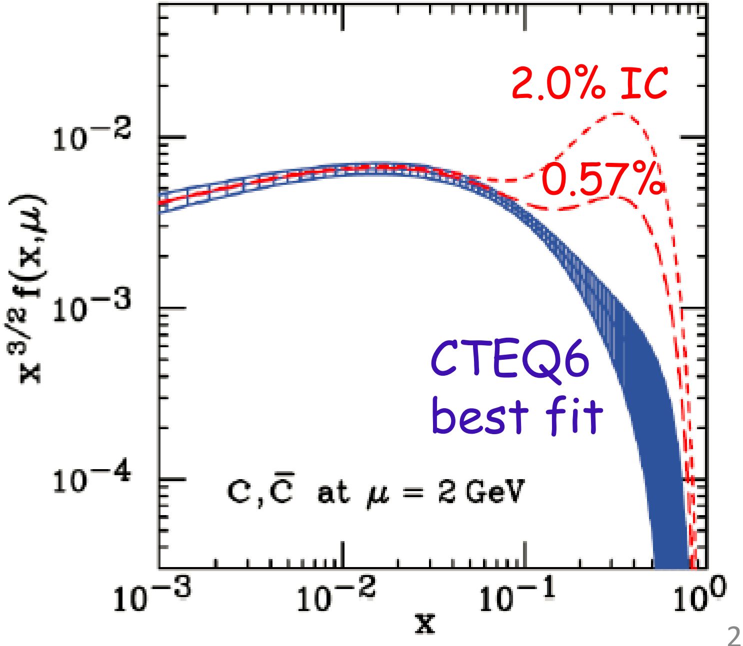

Flattening of shadowing at very small x?

F_2 structure functions (q & qbar) may show leveling out of shadowing at smallest x values probed by DIS on nuclear targets (E665)

hep-ph/0506039

J. Phys. G35, 115010 (2008)

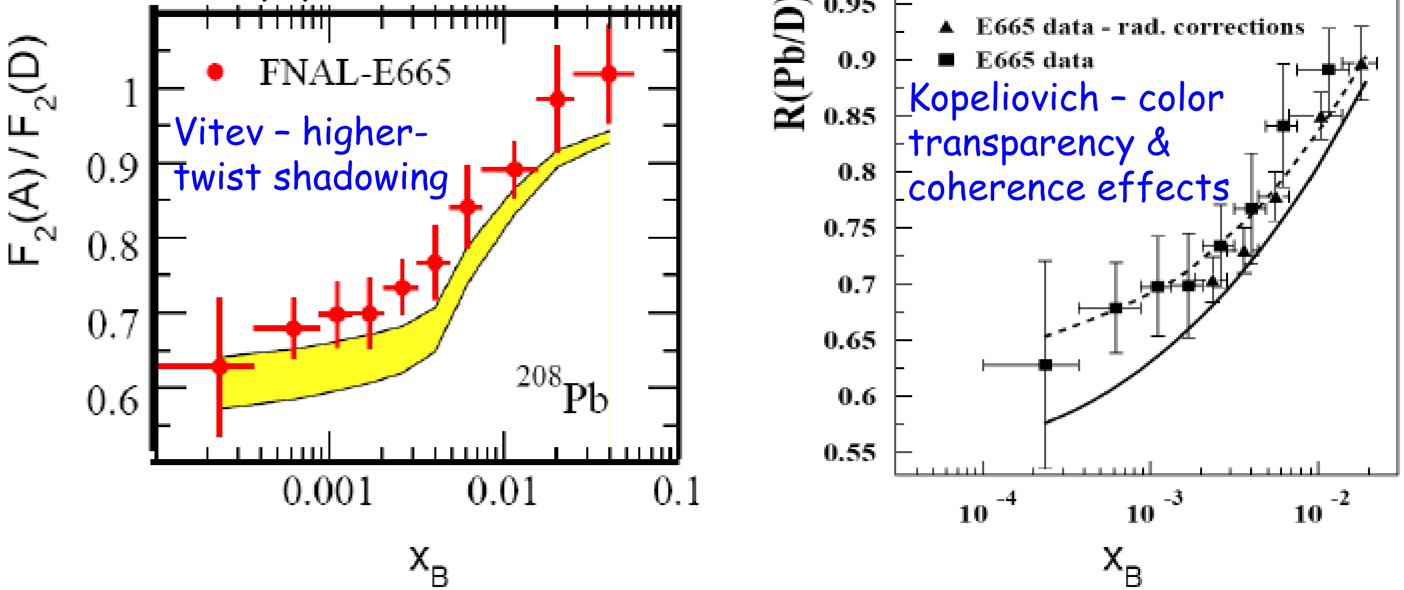

Vitev – higher-twist shadowing

Kopeliovich – color transparency & coherence effects

Figure 3.34: Data from E665 compared with (left) a shadowing calculation from Vitev [307] and with (right) color transparency and coherence calculations from Kopeliovich [223]. In the right panel, the solid (dashed) curve is with (without) the contribution from gluon shadowing.

e.g. probe qbar with very-forward Drell-Yan on nuclear targets

Summary p-A data lessons

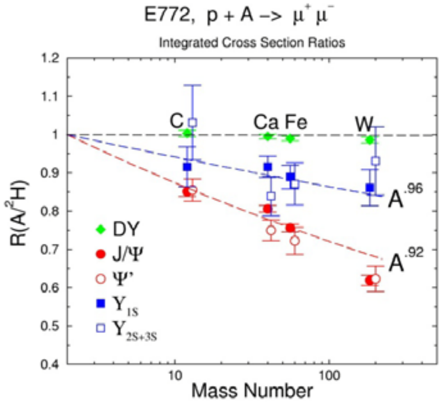

suppression of vector mesons

DY shows shadowing or dE/dx

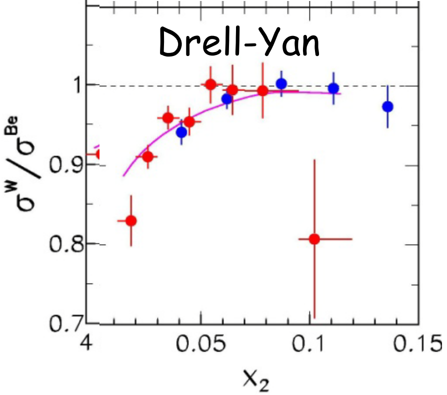

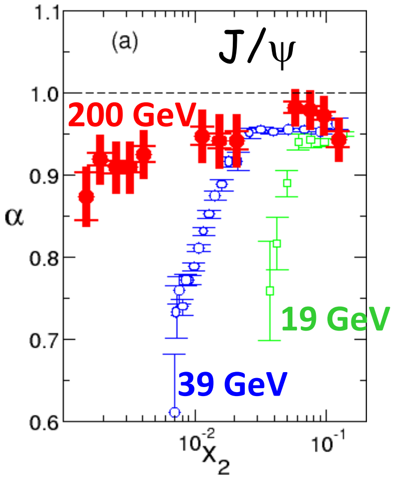

J/ψ suppression doesn't scale like shadowing

Open vs closed charm isolates initial state

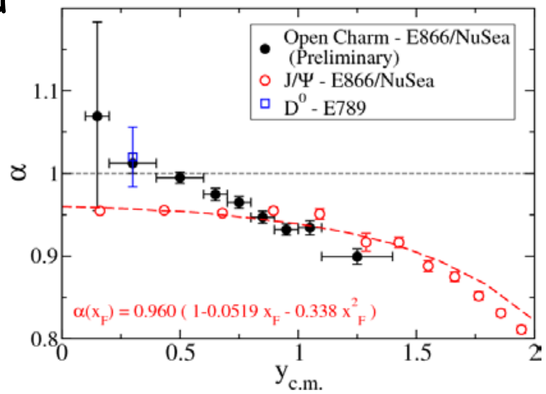

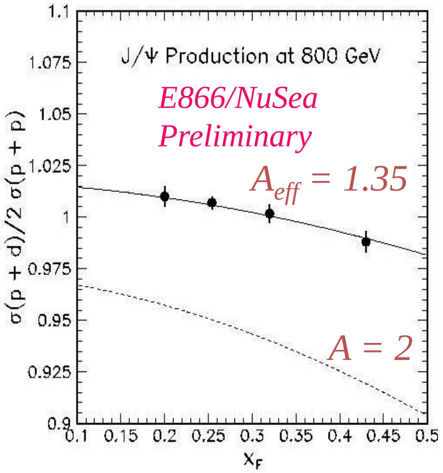

p+d J/ψ suppression is weak

everything has p_T broadening

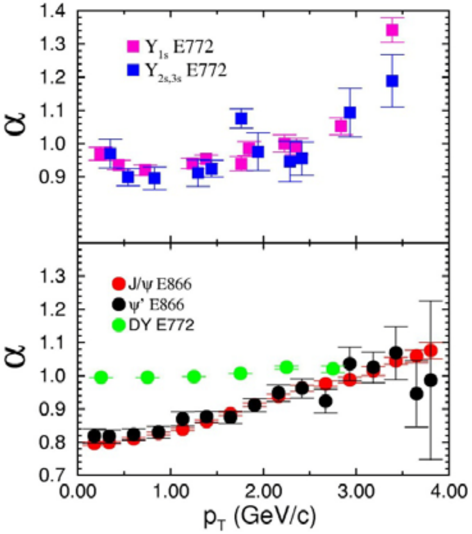

Shadowing may flatten for $x<10^{-3}$?

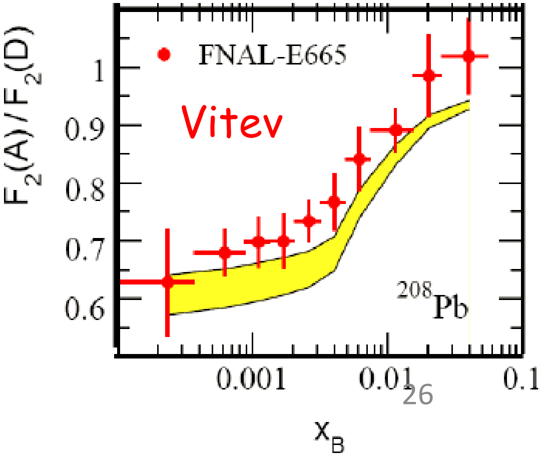

Backups

Solving the J/ψ Puzzle

MJL - 4/3/12

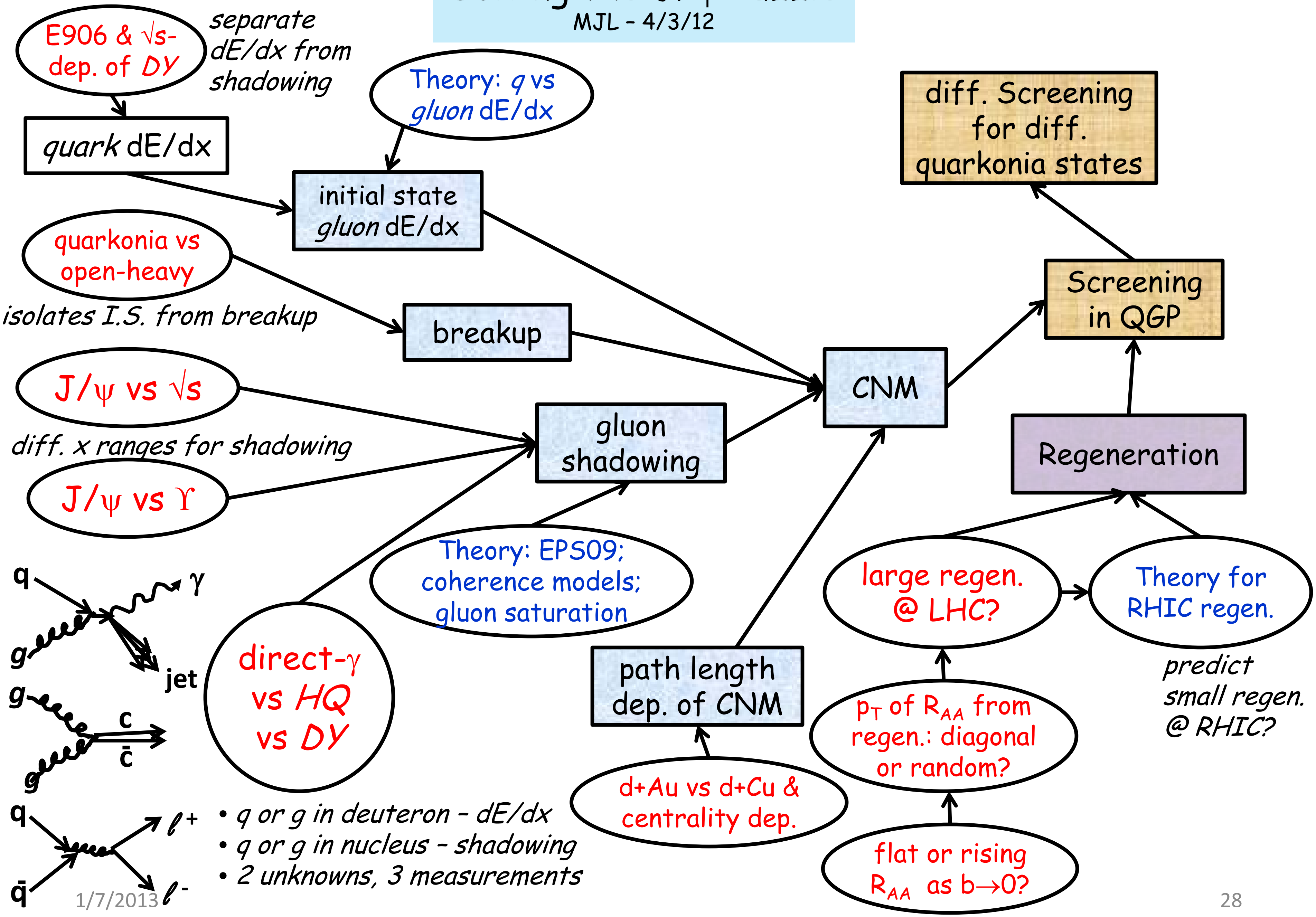

E906 & $\sqrt{s}$-dep. of *DY*

separate dE/dx from shadowing

quark dE/dx

Theory: *q* vs *gluon* dE/dx

initial state *gluon* dE/dx

quarkonia vs open-heavy

isolates I.S. from breakup

breakup

J/ψ vs $\sqrt{s}$

diff. x ranges for shadowing

J/ψ vs Υ

gluon shadowing

Theory: EPS09; coherence models; gluon saturation

direct-γ vs *HQ* vs *DY*

- *q or g in deuteron – dE/dx*
- *q or g in nucleus – shadowing*
- *2 unknowns, 3 measurements*

path length dep. of CNM

d+Au vs d+Cu & centrality dep.

CNM

Screening in QGP

diff. Screening for diff. quarkonia states

Regeneration

large regen. @ LHC?

Theory for RHIC regen.

predict small regen. @ RHIC?

p_T of R_{AA} from regen.: diagonal or random?

flat or rising R_{AA} as $b \to 0$?

HERA-B - J/ψ A dependence

$$\sigma_A = \sigma_N A^{\alpha}$$

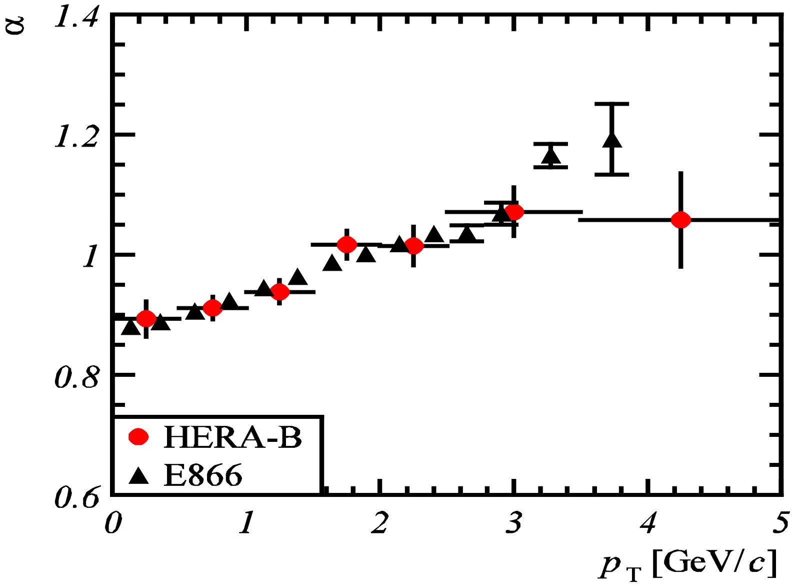

A. Zoccoli (HERA-B) – talk @ Hard Probes 2004

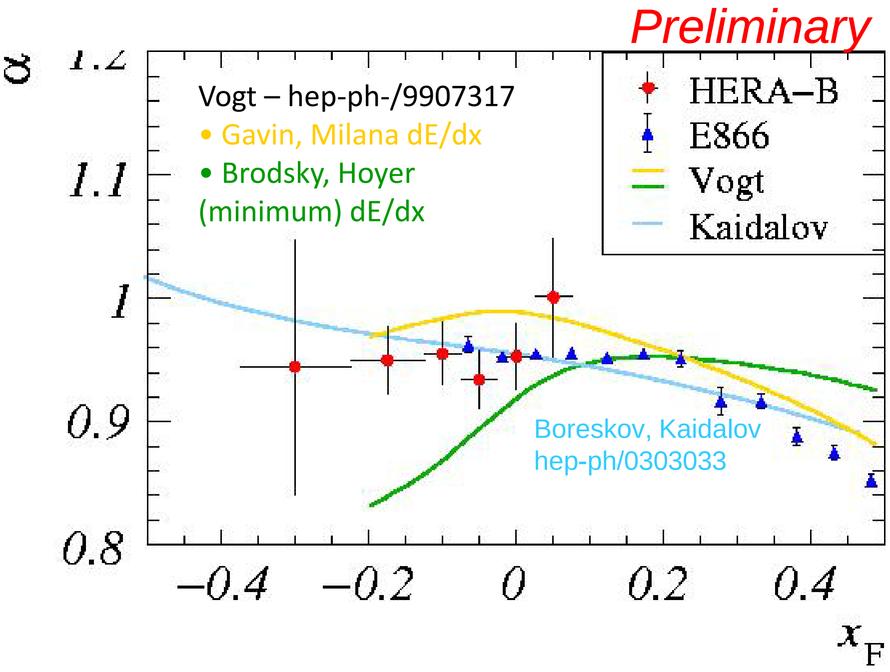

- Previous result of FNAL E866 extended to $x_F = -0.35$
- Result from 15% of full $\mu^+ \mu^-$ sample, statistical uncertainties only, similar results for e^+e^-
- Work on systematics ongoing. Complete the analysis on the full data sample.

Open Charm Nuclear Dependence : x_F Dependence?

E769 250 GeV $\pi^\pm$ PRL 70,722 (1993)

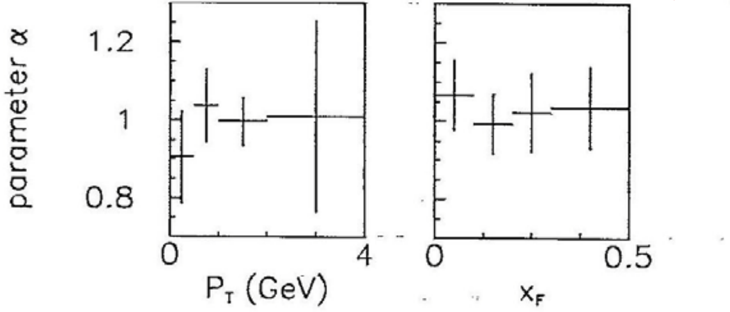

FIG. 4. Dependence of the parameter α on P_T and x_F for D^+ and D^0.

WA82 340 GeV π^- PRB 284,453 (1992)

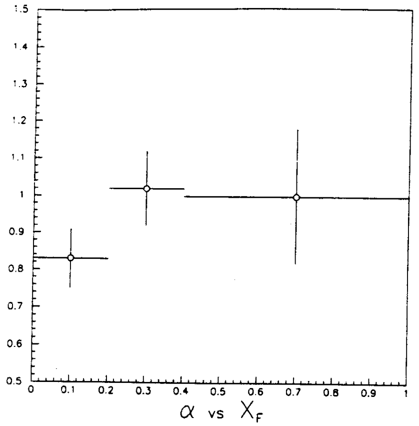

Fig. 4. The parameter α for charm production as measured in three x_F intervals.

Vogt et al., NP 383,643 (1992)

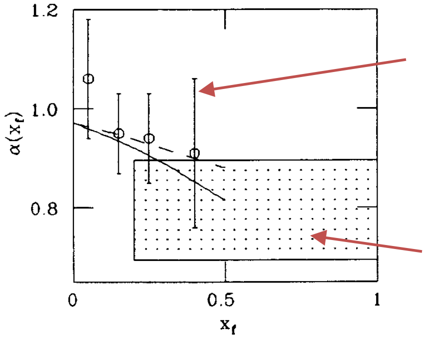

Fig. 14. We show $\alpha(x_f)$ for π^-A interactions at 300 GeV as calculated in our model. The dashed curve shows delta function fragmentation, the solid curve, the Peterson function. These results are compared to those for D$^\pm$ mesons produced by 250 GeV π^-A interactions [3] and the effective α found by the WA78 beam dump experiment [23], indicated by the band with $\langle x_f \rangle = 0.31$.

E769 250 GeV π^-

WA78 320 GeV π^- *(Beam dump)*

What About A-dependence of Drell-Yan??

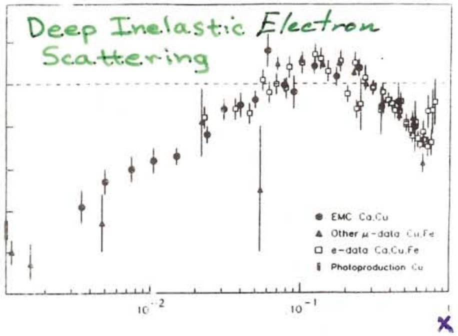

SHADOWING

X < 0.1 quarks suppressed in nuclei.

Gluons probably also suppressed.

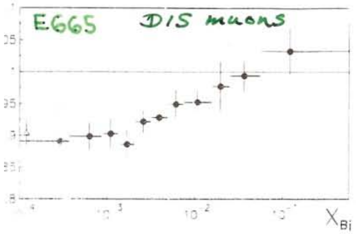

E665
Deep Inelastic Scattering
(470 GeV/c μ)
Z. Phys. C67, 403 (1995)

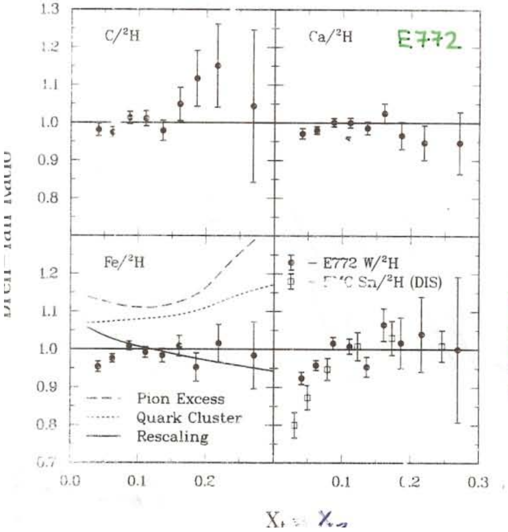

Explains low-x Drell-Yan

E772
$p + A \rightarrow \mu^+\mu^-$
@ 800 GeV/c
PRL 64, 2479 (1990)

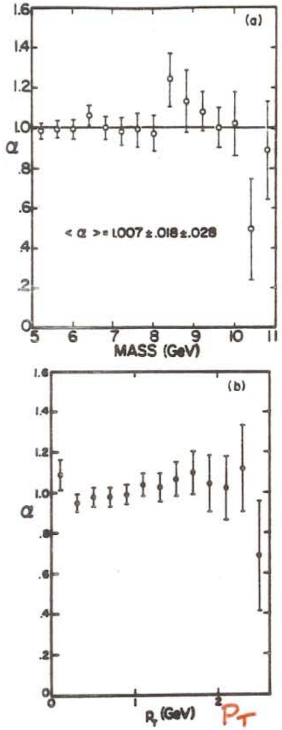

E288 – 400 GeV protons
PRD 23, 604 (1981).

NUCLEAR DEPENDENCE OF DRELL-YAN.

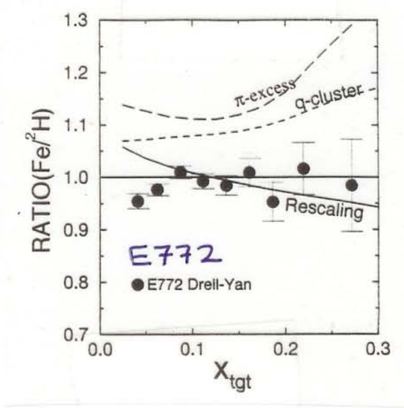

NA10 – 140 GeV/c & 288 GeV/c π^-
PL B 193, 368 (1987).

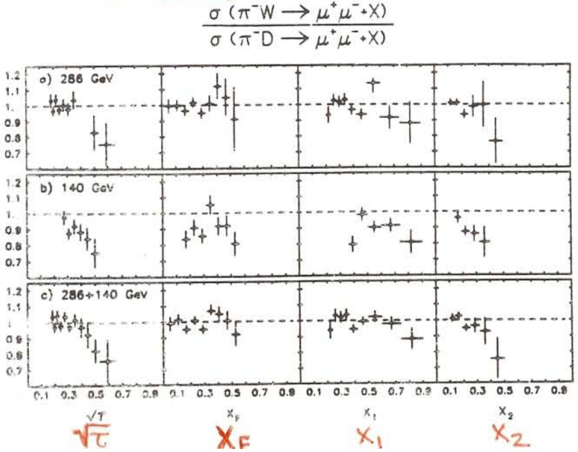

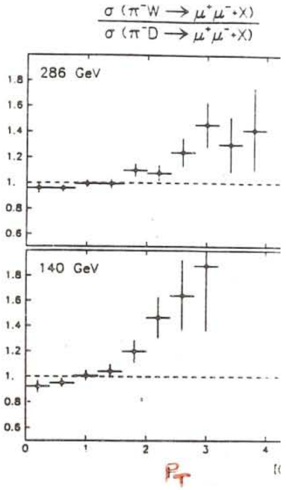

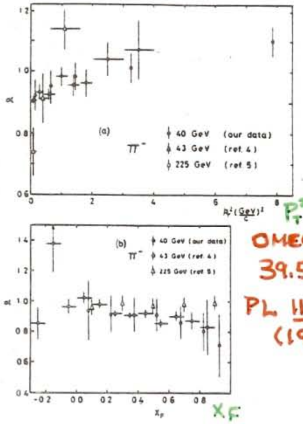

Fig. 3. Variation of A-dependence parameter α, $A^\alpha = \sigma(W)/\sigma(H_2)$, for π⁻ induced J/ψ as a function of p_T^2 and x_F. No corrections have been made for the effects of Fermi motion.

MORE J/ψ
NUCLEAR DEP.

OMEGA Spectr.
39.5 GeV/c π⁻
PL 110B, 415
(1982).

NA3
Z. Phys.
20, 101
(1983).
150 &
200 &
280 GeV/c

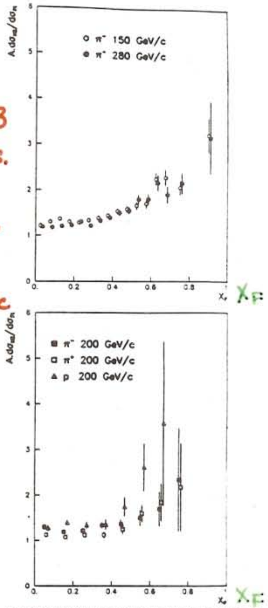

Fig. 2. Ratio of J/ψ cross sections on hydrogen and platinum $R(x_F) = A \frac{d\sigma(H_2)}{dx_F} \Big/ \frac{d\sigma(Pt)}{dx_F}$ for the various π⁺, π⁻, p data of the experiment

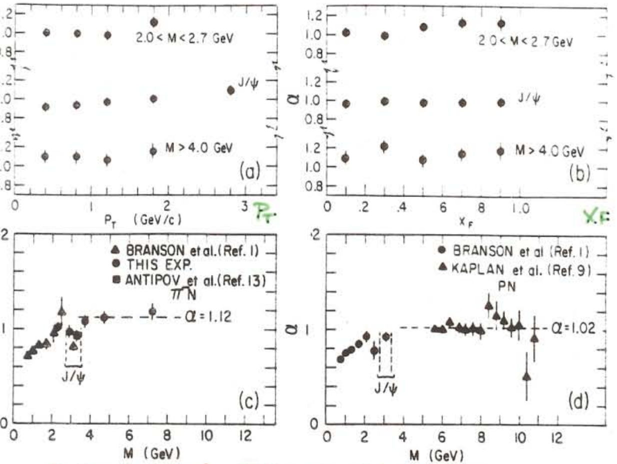

Anderson et al. PRL 42, 944 (1979).
225 GeV/c π±, K⁺, p±

NA38
PL 270, 105
(1991).

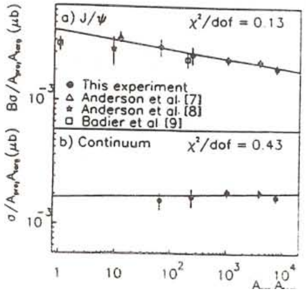

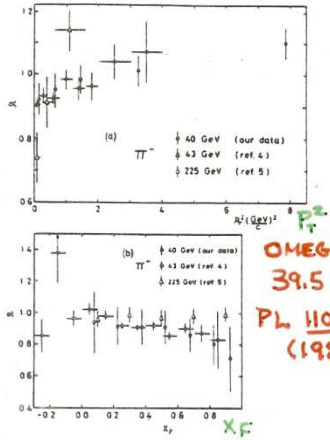

Fig. 3. Variation of A-dependence parameter α, $A^\alpha = \sigma(W)/\sigma(H_2)$, for π⁻ induced J/ψ as a function of p_T^2 and x_F. No corrections have been made for the effects of Fermi motion.

MORE J/ψ
NUCLEAR DEP.

NA3
Z. Phys.
20, 101
(1983).
150 &
200 &
280 GeV/c

OMEGA Spectr.
39.5 GeV/c π⁻
PL 110B, 415
(1982).

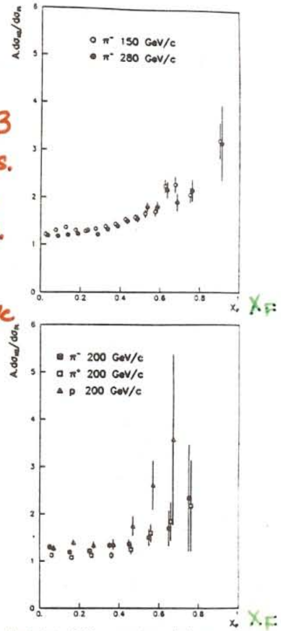

Fig. 2. Ratio of J/ψ cross sections on hydrogen and platinum $R(x_F) = A \frac{d\sigma(H_2)}{dx_F} \Big/ \frac{d\sigma(Pt)}{dx_F}$ for the various π⁺, π⁻, p data of the experiment

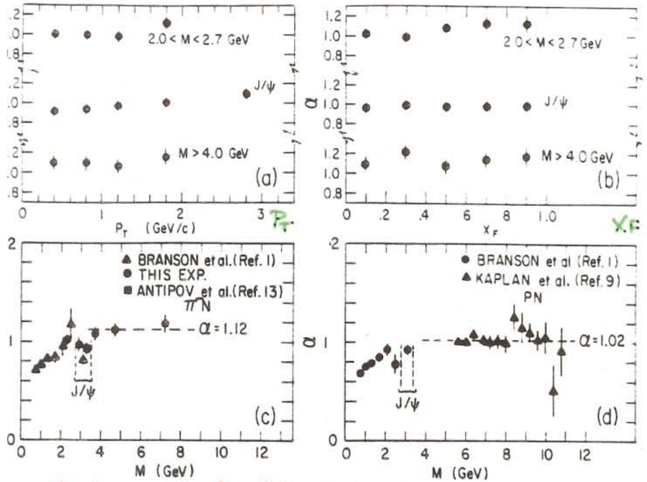

Anderson et al. PRL 42, 944 (1979).
225 GeV/c π±, K⁺, p±

NA38
PL 270, 105
(1991).

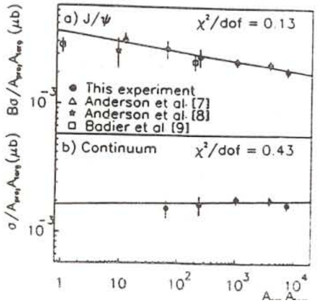

NUCLEAR DEPENDENCE OF J/ψ PRODUCTION

August 28, 1990 V Abramov et al., Fig 6d

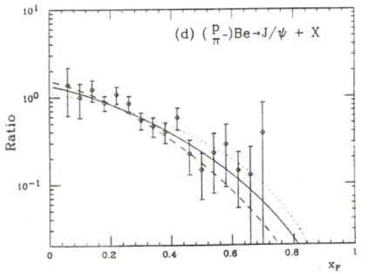

E672/706
530 GeV/c π, p
(FNAL-Pub-91/62-E,
FNAL-Conf-89/151-E)

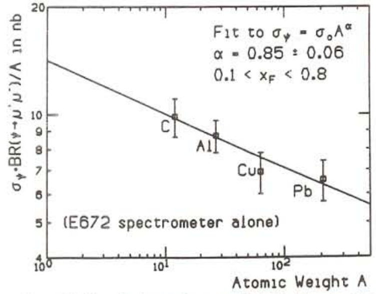

Fig. 7. The A-dependence of J/ψ Production

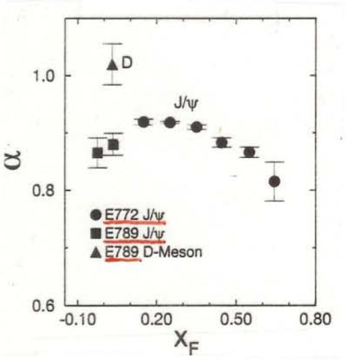

E537
125 GeV/c $\bar{p}$, π^-
PRL 60, 2121 (1988)

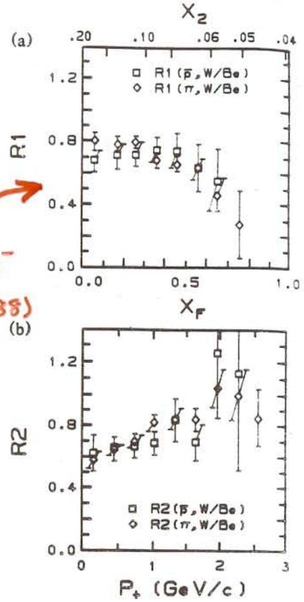

EMC – Theoretical Models

Nuclear Binding & Fermi Motion

(Ericson & Thomas
Bickerstaff & Thomas
Berger & Coester)

Excess pions (nuclear binding)

- Loss of valence quark momentum & enhanced sea (pions)
- Pions have valence (large x) anti-quarks so anti-quark momentum is enhanced

Fermi motion

- Spreads quark momentum near x=1

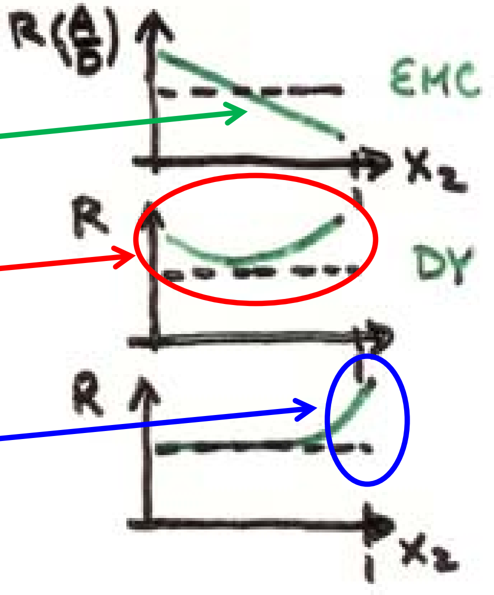

Rescaling (Close et al.; Jaffe)

$$F_2^{Fe}(x,Q^2) \cong F_2^{D}(x,\xi Q^2),\ \ \xi \approx 2$$

~15% phenomological increase in confinement scale

Overlapping nucleons (6-quark clusters, Close, Jaffe,…)

- Loss of valence quark momentum

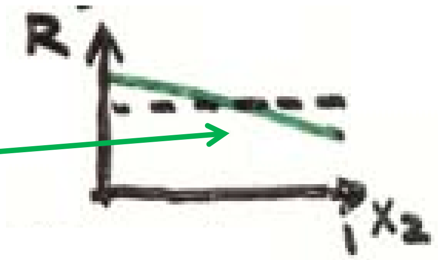

Multi-quark Clusters (Pirner & Vary; Carlson & Havens)

Loss of valence quark momentum

relative enhancement at x~1 (one quark can have > nucleon momentum)

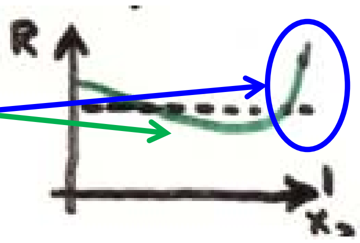

Sudakov suppression

Kopeliovich hep-ph/0501260

Universal suppression at large x_F seen in data for various reactions:

- forward light hadrons, Drell-Yan, heavy flavor
- often attributed to shadowing since x_2 is small

But this common suppression mechanism can also be viewed as Sudakov suppression :

- no particles produced as $x_F \to 1$ due to energy conservation
- more multiple interactions make the effect larger in nuclei

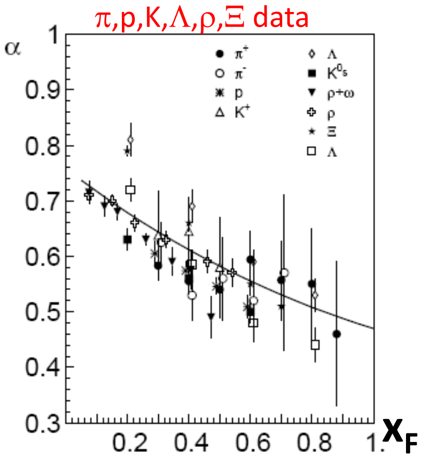

describes universal suppression vs x_F for low energy data

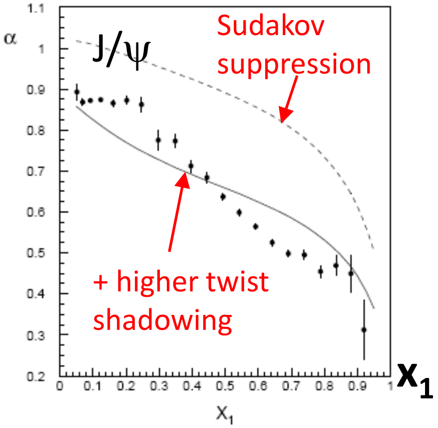

Close to 800 GeV J/ψ suppression vs x_1 ($x_1 \approx x_F$)

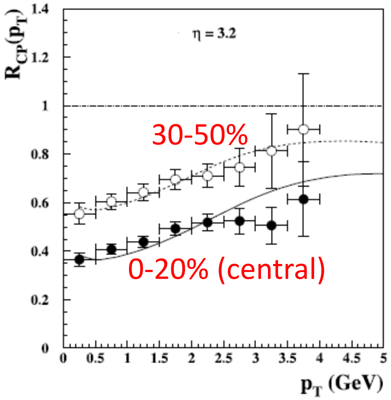

and Brahms forward rapidity (η=3.2) hadrons

Fermilab E866/NuSea Detector

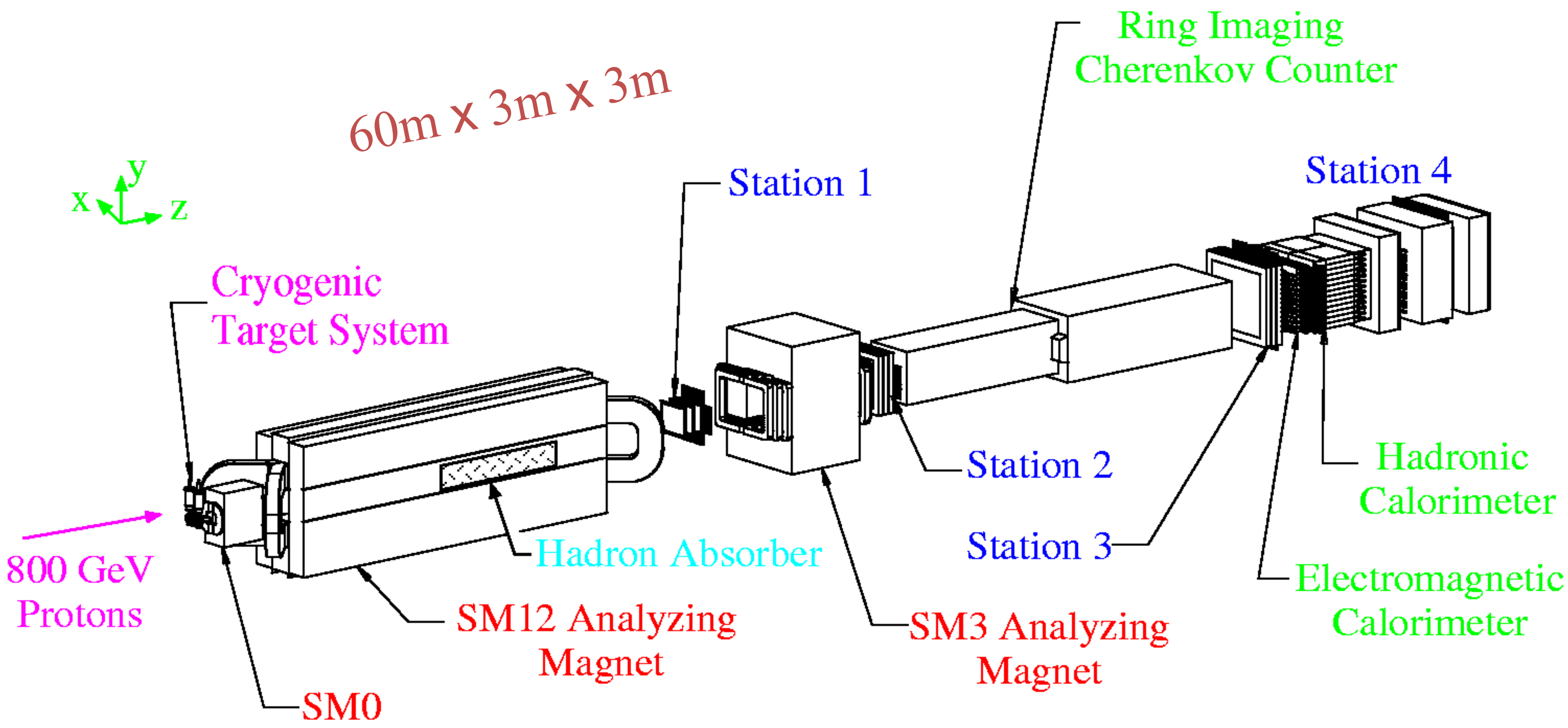

- Forward x_F, high mass μ-pair spectrometer
- Liquid hydrogen and deuterium targets
- Two acceptance defining magnets (SM0, SM12)

- Beam dump (4.3m Cu)
- Hadronic absorber (13.4 I_0-Cu, C, CH_2)
- Momentum analyzing magnet (SM3)
- Three tracking stations
- Muon identifier wall & 4th tracking

NA38/NA50

Luminosity monitor

EmCAL, ZDC, Si-strip multiplicity detector for centrality determination

Toroidal analyzing magnet

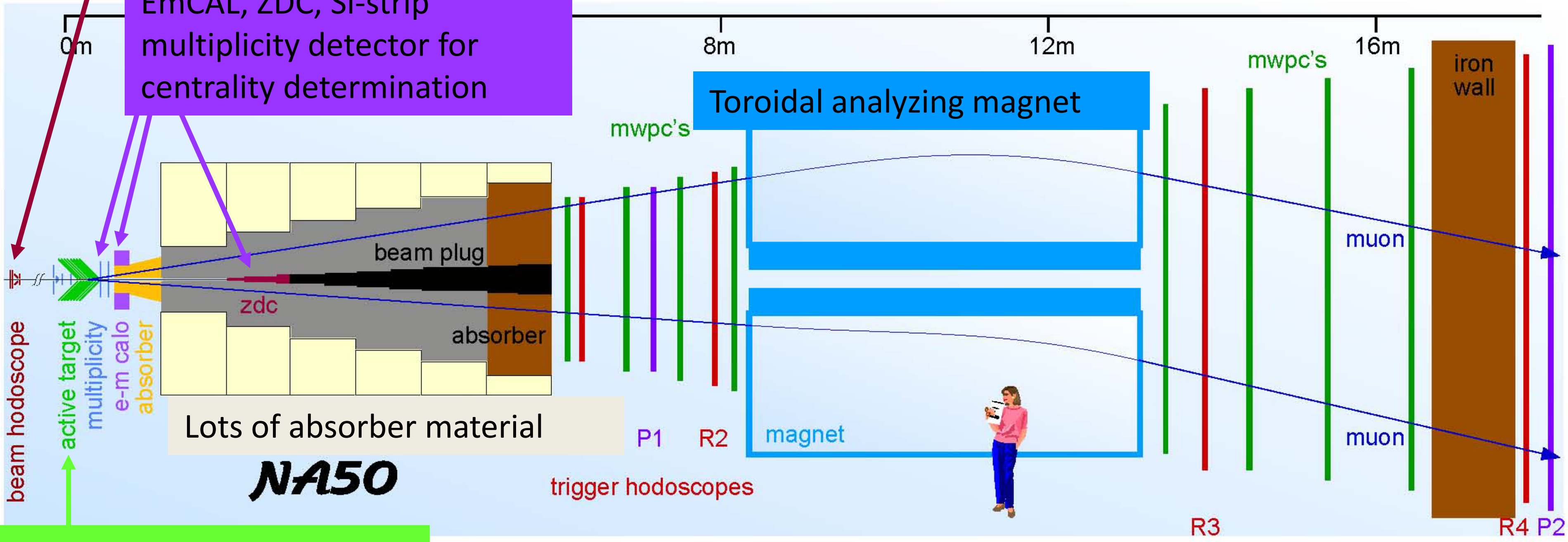

Lots of absorber material

Segmented active target

MWPCs, hodoscopes for tracking/triggering

Note benefits of a fixed target experiment:

- Lots of luminosity.
- Boost in lab frame gives very high momentum particles, so resolution is improved and background can be greatly reduced by many meters of absorber.

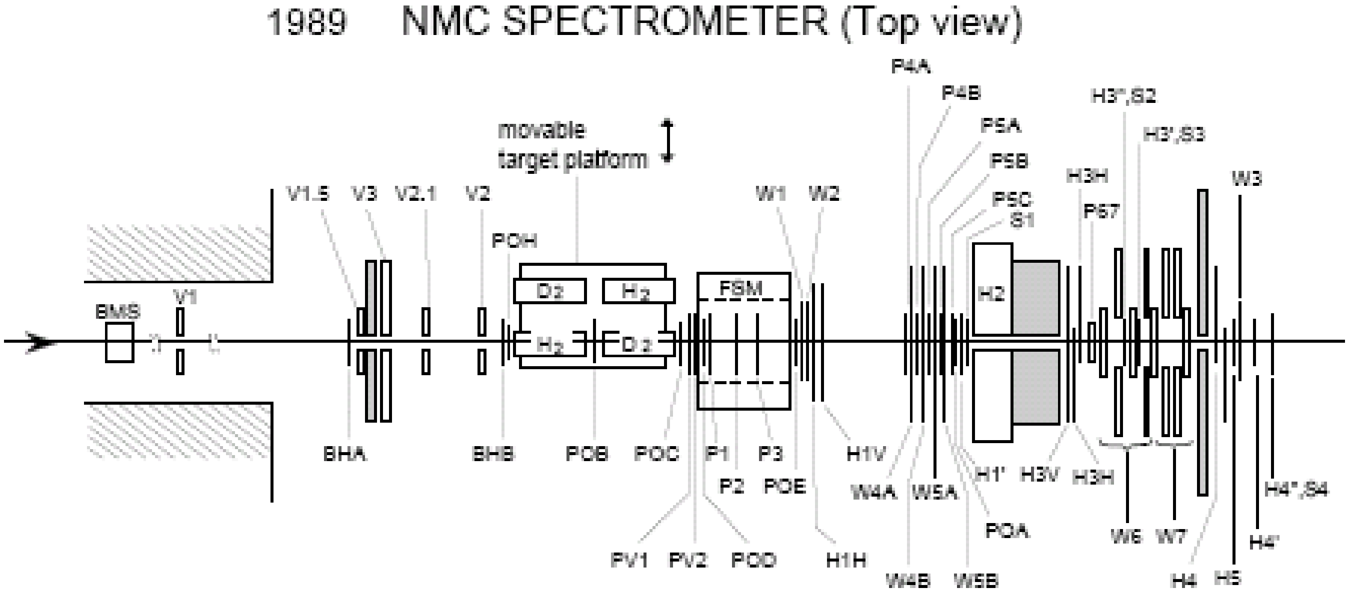

BMS	Beam momentum spectrometer
V1, V1.5, V3, V2.1, V2	Veto counters
BHA, BHB	Beam hodoscopes
POA–E,POH, PV1–2, P1–3, P4A–5C,P67	Proportional chambers
FSM	Forward spectrometer magnet
W1–3, W4A–5B, W6–7	Drift chambers
H1H, H1V, H3V, H3H, H4, H5	Large angle trigger (T1) hodoscopes
H1', H3', H4'	Small angle trigger (T2) hodoscopes
S1–4, H3", H4"	Small x trigger (T14) hodoscopes
H2	Hadron calorimeter
▨	Iron absorbers

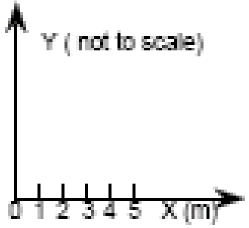

Figure 1: The NMC spectrometer for the 1989 data taking. The beam calibration spectrometer is located downstream and not shown.

The HERA-B Detector

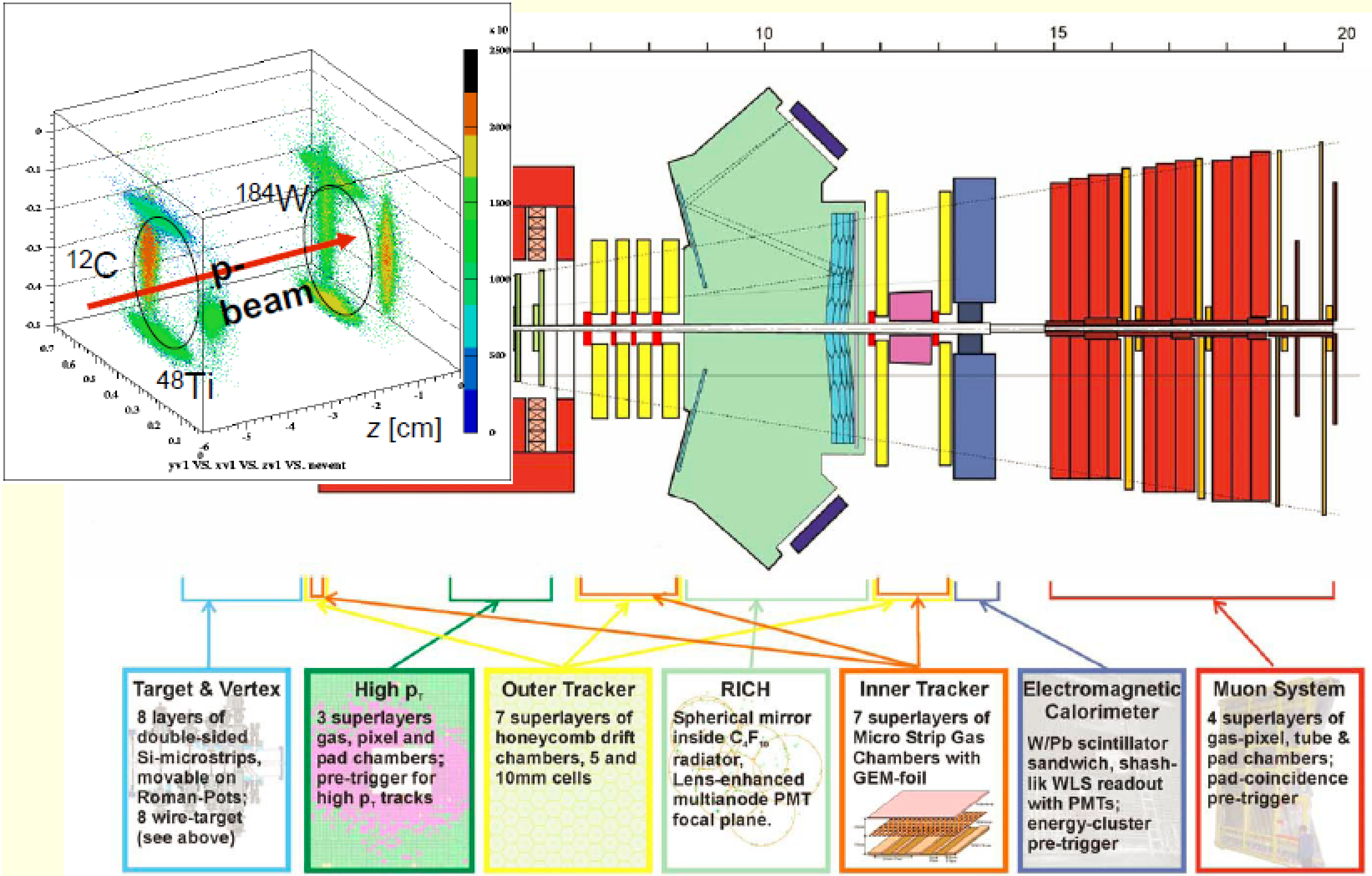

Target & Vertex
8 layers of double-sided Si-microstrips, movable on Roman-Pots; 8 wire-target (see above)

High p_T
3 superlayers gas, pixel and pad chambers; pre-trigger for high p_T tracks

Outer Tracker
7 superlayers of honeycomb drift chambers, 5 and 10mm cells

RICH
Spherical mirror inside C_4F_{10} radiator, Lens-enhanced multianode PMT focal plane.

Inner Tracker
7 superlayers of Micro Strip Gas Chambers with GEM-foil

Electromagnetic Calorimeter
W/Pb scintillator sandwich, shashlik WLS readout with PMTs; energy-cluster pre-trigger

Muon System
4 superlayers of gas-pixel, tube & pad chambers; pad-coincidence pre-trigger

Production of hadrons at large transverse momentum at 200, 300 and 400 GeV at Fermilab

J.W. Cronin et al., PRD 11, 3105 (1975)

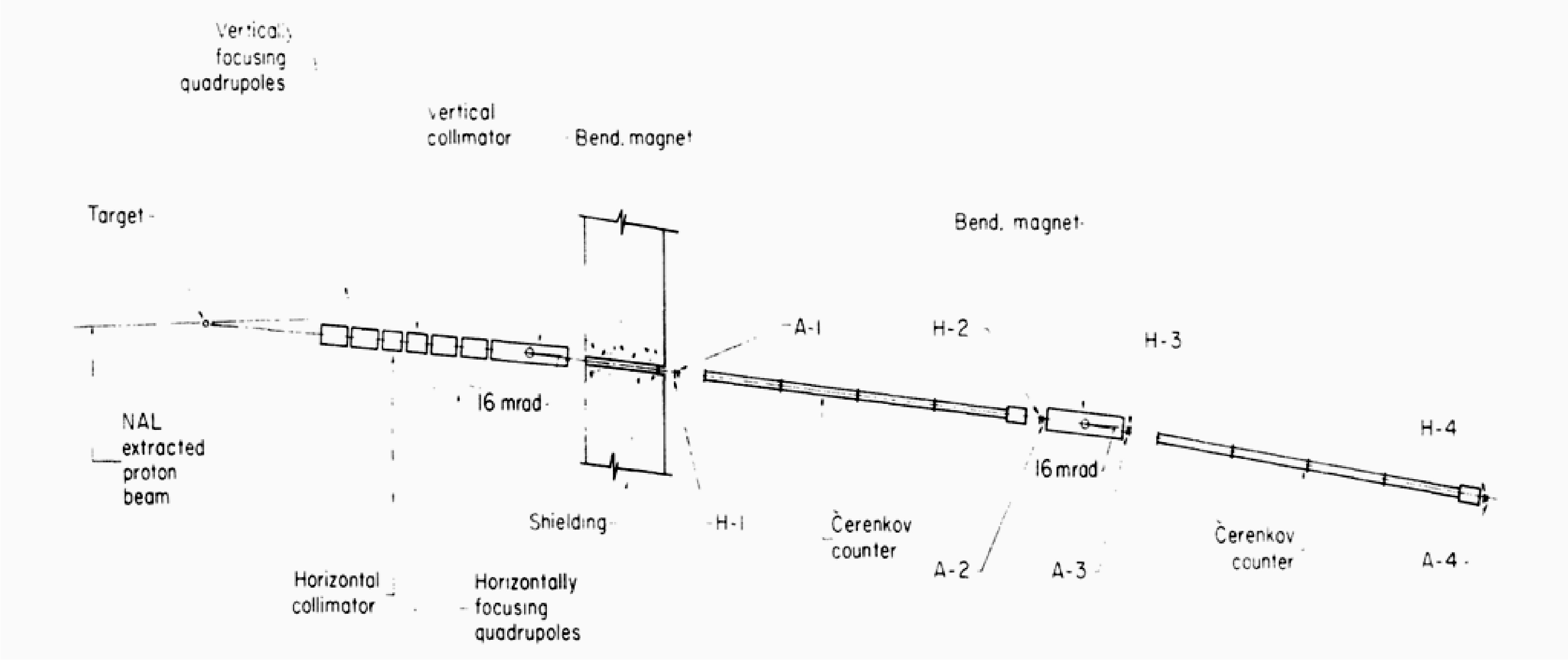

A Dependence of J/ψ and ψ' Not Identical: Size Matters

Color octet mechanism suggested that J/ψ and ψ' A dependence should be identical — Supported by large uncertainties of early data

More extensive data sets (NA50 at SPS, E866 at FNAL) show clear difference at midrapidity [NA50 ρL fit gives $\Delta\sigma = \sigma_{\rm abs}^{\psi'} - \sigma_{\rm abs}^{J/\psi} = 4.2 \pm 1.0$ mb at 400 GeV, 2.8 ± 0.5 mb at 450 GeV for absolute cross sections]

Suggests we need to include formation time effects

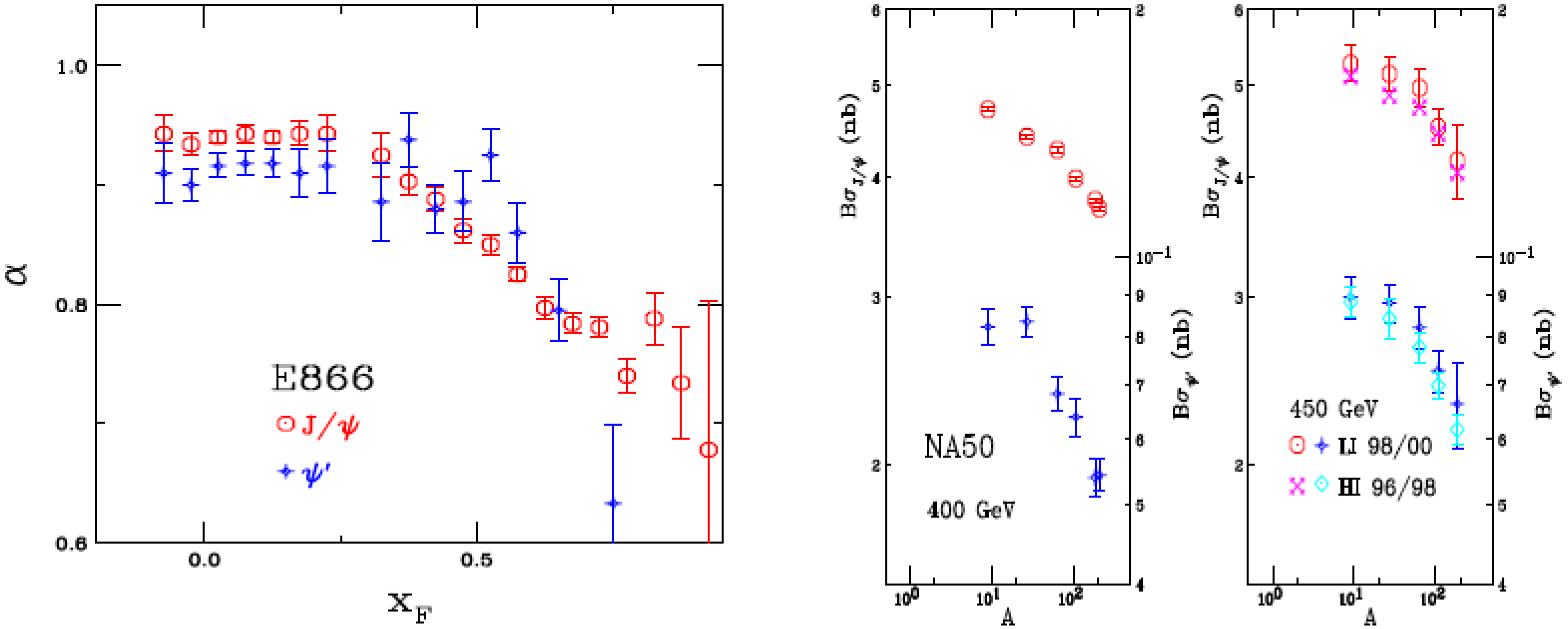

Figure 15: The J/ψ A dependence (left) as a function of x_F at FNAL ($\sqrt{s_{NN}} = 38.8$ GeV) and (right) and a function of A at the SPS (NA50 at $p_{\rm lab} = 400$ and 450 GeV) for J/ψ and ψ' production.

slide from R. Vogt – Jan. 2011

Quark Energy Loss from Drell-Yan data assuming EKS Shadowing

Parton energy loss limits

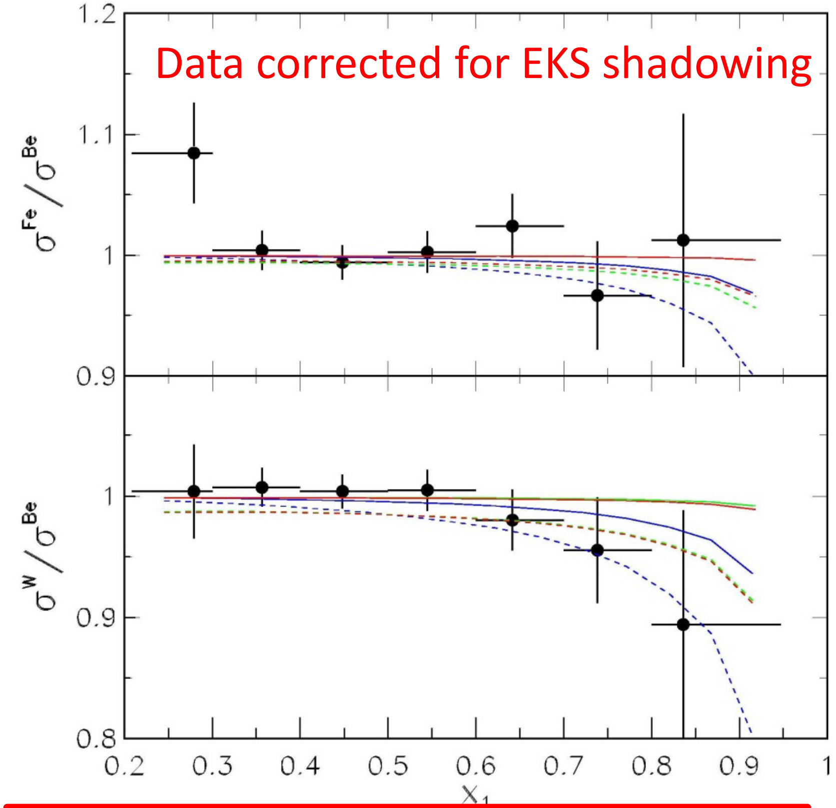

Data corrected for EKS shadowing

- Gavin and Milana $\Delta E < 0.14\,\%/\mathrm{fm}$
- Brodsky and Hoyer $\Delta E < 0.44\,\mathrm{GeV/fm}$
- Baier et al. $\Delta E < (0.046\,\mathrm{GeV/fm}^2) \times L^2$

Phys. Rev. Lett. 83, 2304 (1999)

- S.Gavin, J.Milana, Phys.Rev.Lett 68(1992)1834

$$\Delta x_1 = kCx_1\left(\frac{Q_0}{Q}\right)^n A^{\frac{1}{3}}$$

$C = 4/3$ for quarks, $C = 3$ for gluons, $n =$ for ”soft physics” Experimental fit: $\Delta x_1 = -k_1 x_1 A^{\frac{1}{3}}$

- S.Brodsky, R.Hoyer, Phys.Lett. B298(1993)165

$$|\Delta x_1| \leq \frac{< k_\perp > L_a}{2E}$$

Experimental fit: $\Delta x_1 = -\frac{k_2}{s} A^{\frac{1}{3}}$

- R.Baier et al., Nucl.Phys. **B**484(1997)265
  R.Baier et al., Nucl.Phys. **B**531(1998)403

$$|\Delta x_1| = \frac{3\alpha_s}{2}\frac{m_p}{s} L_a < p_\perp^2 >$$

Experimental fit: $\Delta x_1 = -\frac{k_3}{s} A^{\frac{2}{3}}$

Quark Energy Loss from Drell-Yan data assuming Kopeliovich Shadowing

Johnson, Kopeliovich et al., PRL 86, 4483 (2001)

data from
E772 - PRL 64, 2479 (1990)

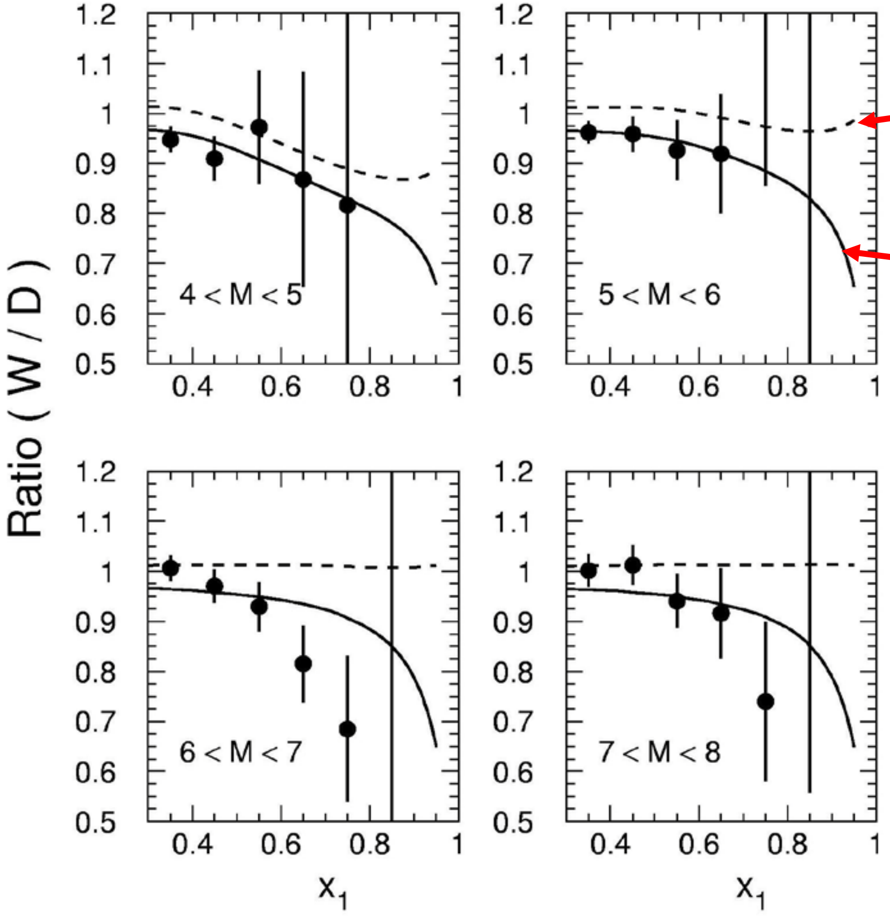

Shadowing

dE/dx
+ Shadowing

Analysis of our p-A Drell-Yan data using the Kopeliovich model. Dashed lines with shadowing only; solid lines with parton energy loss of

$dE/dx = 2.32 \pm 0.52 \pm 0.5$ GeV/fm

Confusion due to having both shadowing and dE/dx contributing to Drell-Yan suppression for measurements at this energy

Intrinsic charm contribution to Quarkonia

At large x_F (≥ 0.5) intrinsic $c\bar{c}$ components of the projectile proton can dominate the production of charm pairs

- $A^{2/3}$ dependence via surface stripping of light quarks to free charm pair component

Vogt, Brodsky, Hoyer, NP B360, 67 (1991)
(also includes absorption and shadowing)

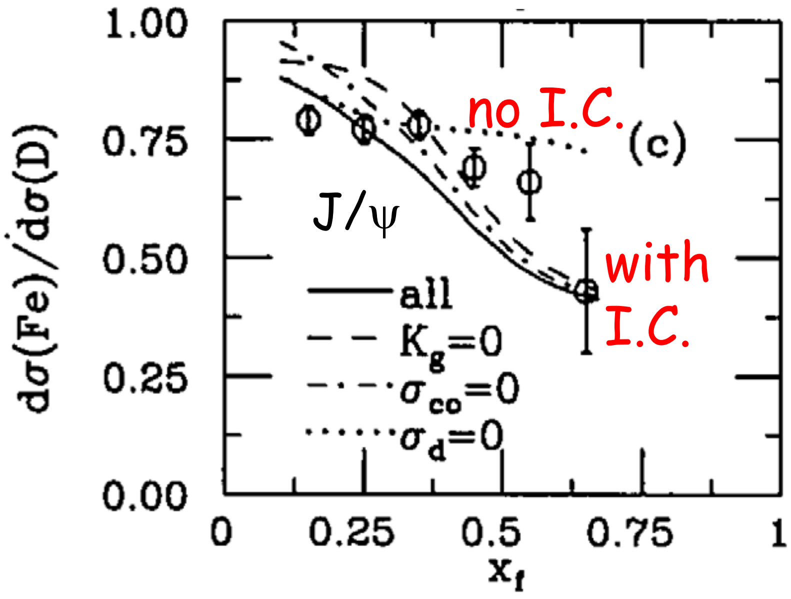

But E789 set limit on I.C. contribution via shape of cross section vs x_F

- $< 2.3 \times 10^{-3}$ nb/nucleon (1.8 nb/nucleon predicted)

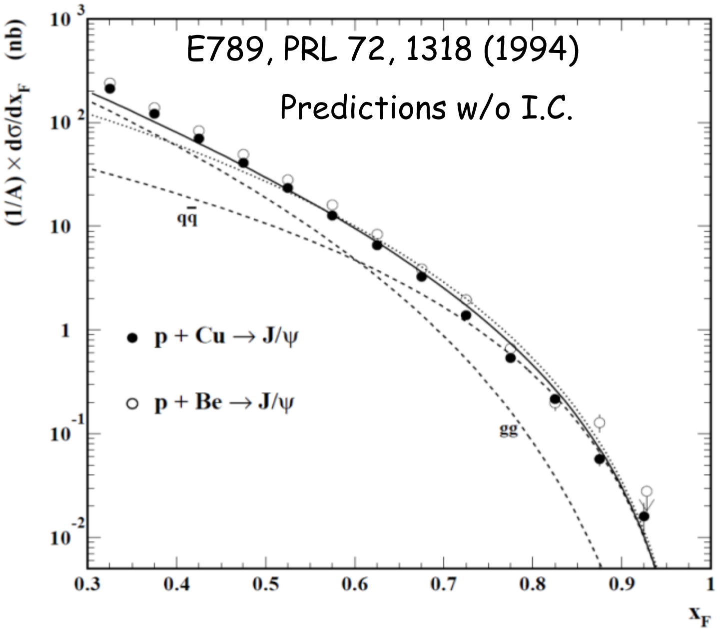
E789, PRL 72, 1318 (1994)

Predictions w/o I.C.

“Evidence” for the “intrinsic” charm (IC)

DIS data

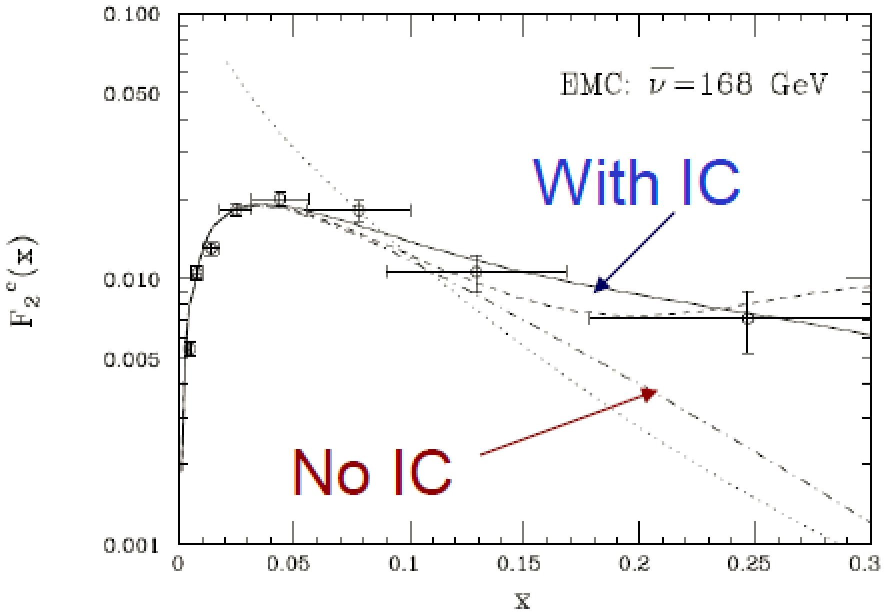

Λ_c production

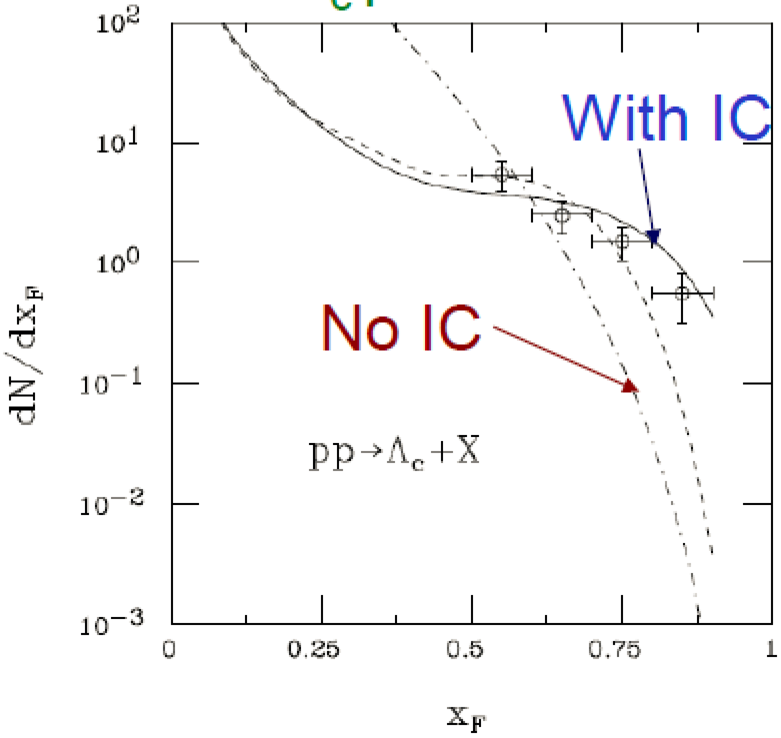

Gunion and Vogt (hep-ph/9706252)

“Evidence” appears to be rather weak

Slide from JCP

No conclusive experimental evidence for intrinsic-charm

PHYSICAL REVIEW D 75, 054029 (2007)

Charm parton content of the nucleon

J. Pumplin,[1,*] H. L. Lai,[1,2,3] and W. K. Tung[1,2]

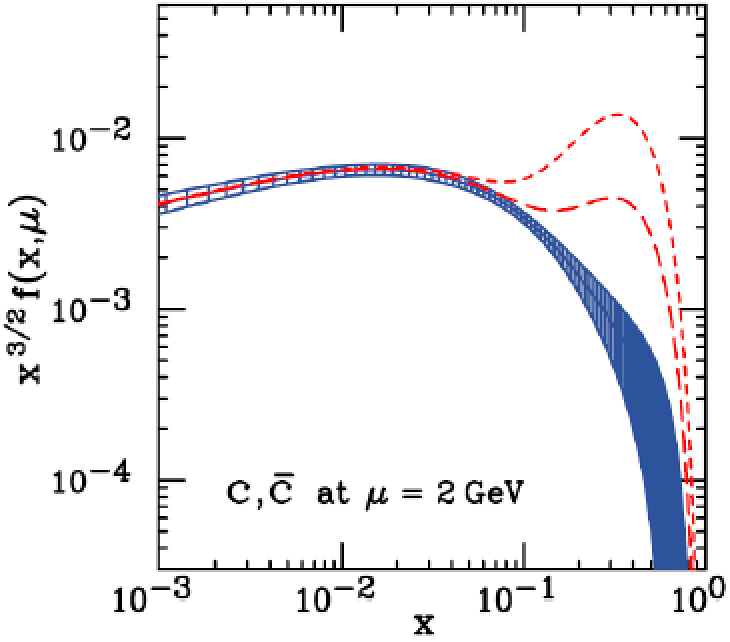

Blue band corresponds to CTEQ6 best fit, including uncertainty

Red curves include intrinsic charm of 0.57% and 2.0%

We find that the range of IC is constrained to be from zero (no IC) to a level 2–3 times larger than previous model estimates. The behaviors of typical charm distributions within this range are described, and their implications for hadron collider phenomenology are briefly discussed.

Slide from JC Peng